

IMAGING THROUGH OBSCURATIONS FOR SLUICING  
OPERATIONS IN THE WASTE STORAGE TANKS

T. J. Peters  
D. L. McMakin  
D. M. Sheen  
M. A. Chieda

August 1994

Prepared for  
the U.S. Department of Energy  
under Contract DE-AC06-76RLO 1830

Funded by the Office of Technology Development,  
within the Department of Energy's Office of Environmental  
Management, under the Characterization, Monitoring and Sensor  
Technology Integrated Program

Pacific Northwest Laboratory  
Richland, Washington 99352

REPRODUCTION OF THIS DOCUMENT IS UNLIMITED

72

MASTER

## Acknowledgements

This work was prepared with the support of the following contributors:

Headquarters: Office of Technology Development  
Characterization, Monitoring & Sensor  
Technology Integrated Program  
Caroline Purdy

Operations Office: Richland Operations Office  
Technology Development Division  
Deborah E. Trader, Technical Program Officer

Contractor: Pacific Northwest Laboratory  
Environmental Management Directorate  
Steven C. Slate, Technical Program Manager

## **DISCLAIMER**

**This report was prepared as an account of work sponsored by an agency of the United States Government. Neither the United States Government nor any agency thereof, nor any of their employees, make any warranty, express or implied, or assumes any legal liability or responsibility for the accuracy, completeness, or usefulness of any information, apparatus, product, or process disclosed, or represents that its use would not infringe privately owned rights. Reference herein to any specific commercial product, process, or service by trade name, trademark, manufacturer, or otherwise does not necessarily constitute or imply its endorsement, recommendation, or favoring by the United States Government or any agency thereof. The views and opinions of authors expressed herein do not necessarily state or reflect those of the United States Government or any agency thereof.**

## **DISCLAIMER**

**Portions of this document may be illegible in electronic image products. Images are produced from the best available original document.**

## SUMMARY

This report describes the results of tests conducted at the Pacific Northwest Laboratory (PNL) to determine which methods could be used to obtain an image inside a waste tank during sluicing operations. During waste tank remediation efforts, fog and water droplets that contain salt crystals and/or dust are present which would obscure viewing of the operation. A test chamber was built that allowed various waste remediation conditions, such as size of droplets and salt concentration in waste droplets, to be simulated. The droplets ranged from 25 microns to 1100 microns in diameter, and the salt concentration ranged from 0%-20% by weight. Radiation found in the waste tanks was not simulated, but the effect of radiation on the operation of the devices is discussed in this report.

Three basic imaging techniques were evaluated: optical, acoustic and radar. The optical imaging methods that were examined used cameras which operated in the visible region (0.4-0.8 microns) and near-infrared region (less than two microns) and infrared cameras which operated in the 3-5 micron and 8-12 micron wavelength regions. Various passive and active lighting schemes were tested, as well as the use of filters to eliminate reflection in the visible region. Image enhancement software was used to extend the range where visual techniques could be used. In addition, the operation of a laser range finder, which operated at 0.835 microns, was tested when fog/water droplets were suspended in the air. The acoustic technique involved using commercial acoustic sensors, operating at approximately 50 kHz and 215 kHz, to determine the attenuation of the acoustic beam in a high-humidity environment. The radar imaging methods involved performing millimeter wave (94 GHz) attenuation measurements in the various simulated sluicing environments and performing preliminary experimental imaging studies using a W-Band (75-110 GHz) linearly scanned transceiver in a laboratory environment.

The results of the tests indicate that sensors operating with millimeter waves (94 GHz) were best able to penetrate the fog/water droplets. Signal loss ranged from 0.015 db/ft in 25-micron diameter fog to 0.110 db/ft for 1100-micron diameter water particles. Signals were measured 30-40 db above

noise, using a high-reflecting target. The antenna used for these tests was small, approximately 1 (d) x 1 (w) x 3 (l) inch. In this program, it was demonstrated that a scanner could be used to create an image using this small antenna. The millimeter wave beam was not affected by adding salt to the water.

Acoustic sensors that operated at 50 kHz would be affected by the noise in the sluicing operation. Acoustic sensors that operated at 215 kHz were not as affected by noise, but were highly attenuated in the fog/water droplets (0.071 db/ft. in fog, which means the power level would decrease by 75% travelling to and from a target at 80 feet). Acoustic sensors were not affected by the addition of salt to the fog/water droplets.

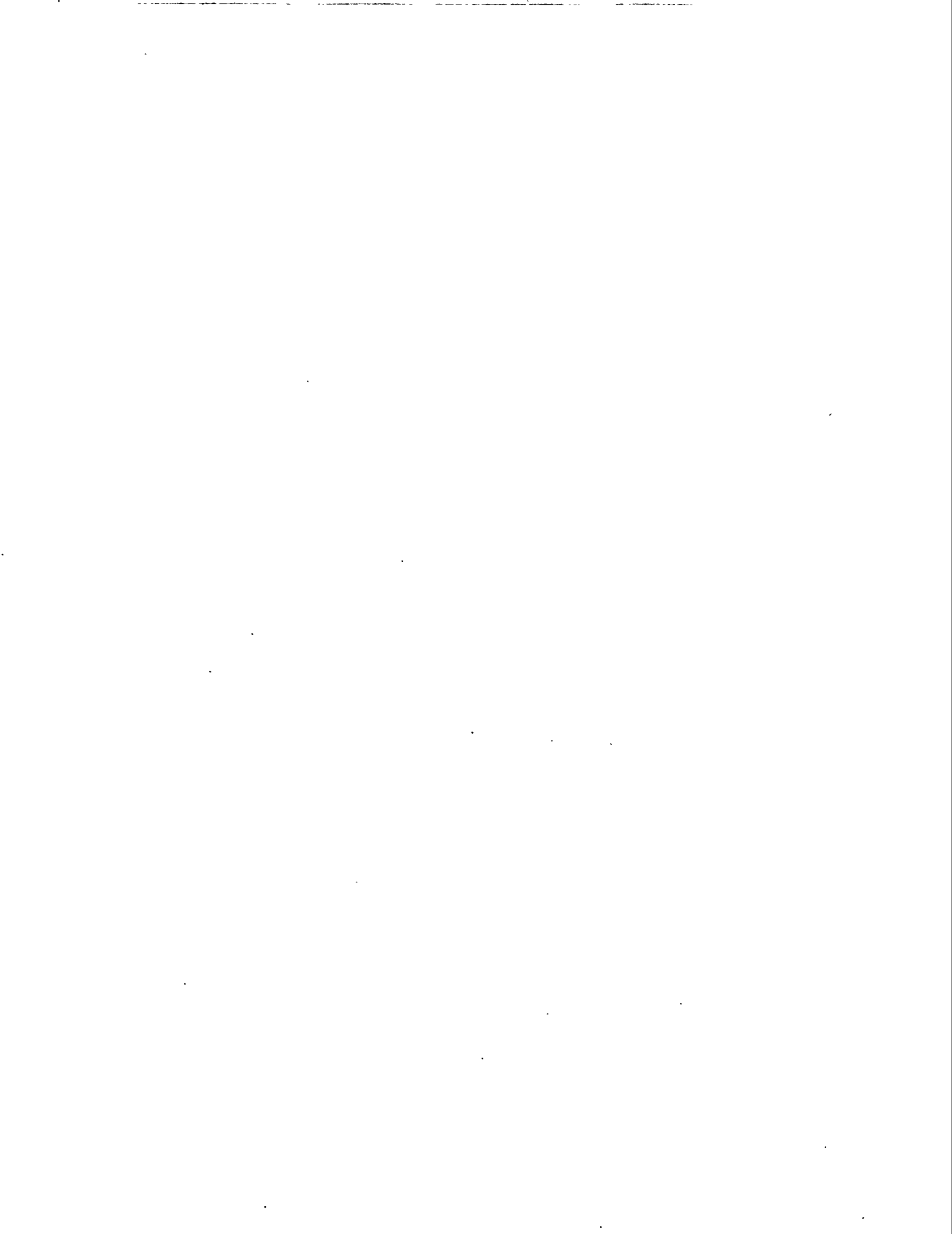
A video system is probably the least expensive and would require the least amount of technical development to meet the viewing needs for the sluicing operation. However, testing indicated that optical techniques were highly attenuated by the fog/water droplets. Although infrared detectors, both in the 2-5 micron and 8-12 micron wavelength regions, were able to view through fog better than visual (0.4-0.7 microns) techniques, infrared imaging systems exhibited higher attenuation with water droplets than imaging systems operating in the visible region. A liquid nitrogen cooled infrared detector is able to view through fog/water droplets that are 25%-200% more dense than a thermoelectric-cooled detector (for a target at 83°F). However, a liquid nitrogen cooled infrared detector would be more difficult to implement in a waste tank environment. In addition, the temperature difference between the target area and the background may be small in a closed waste tank environment, which could result in a false image of the area being examined. These results indicate that infrared imaging may not be suitable for viewing through fog/water droplets during a sluicing operation.

Visible techniques can be enhanced by placing the lighting near the area to be viewed (frontlighting), instead of lighting from the camera plane (backlighting). Backlighting produces backscatter from the fog/water droplets which severely reduces contrast in the image. The thicker the fog/water

droplets, the more that is gained by frontlighting. There was no gain in using infrared filters to decrease the backscatter in the visible region from the fog/water droplets. Video imaging can also be enhanced by image enhancement software. The density of the fog that can be viewed with video imaging techniques can be 9% to 42% greater, depending on the lighting scheme, if contrast enhancement techniques are used. This type of image processing can be done in real-time.

A laser range finder lost its ability to determine range through the fog/water droplets due to backscatter. However, by scanning the laser range finder, an image of the target could be obtained through the fog, even though it was a poorer quality compared to other techniques. In water droplets, an image could be obtained using the laser range finder only if the water droplets were at least 16 feet from the laser range finder.

The results of this program will form a basis for making intelligent decisions on which method can be used to view through obscurants during a sluicing operation. In order to make these decisions, it is necessary to define the conditions in the waste tank, e.g., the density of the fog/water droplets. With this information, imaging systems can be developed for specific applications.



## CONTENTS

|                                                            |     |
|------------------------------------------------------------|-----|
| SUMMARY . . . . .                                          | iii |
| 1.0 BACKGROUND . . . . .                                   | 1   |
| 2.0 REVIEW OF CANDIDATE METHODS . . . . .                  | 7   |
| 3.0 TEST RESULTS . . . . .                                 | 11  |
| 3.1 TEST SET-UP . . . . .                                  | 11  |
| 3.2 DISCUSSION OF TESTS . . . . .                          | 19  |
| 3.2.1 Optical Sensors . . . . .                            | 19  |
| Test Results . . . . .                                     | 22  |
| Reproducibility of Results . . . . .                       | 34  |
| 3.2.2 Acoustic Sensors . . . . .                           | 34  |
| Test Results . . . . .                                     | 36  |
| 3.2.3 Wideband Millimeter Wave Imaging Technique . . . . . | 38  |
| Test Results . . . . .                                     | 39  |
| Attenuation Measurements . . . . .                         | 39  |
| Imaging Tests . . . . .                                    | 42  |
| Conceptual Design . . . . .                                | 45  |
| 4.0 RADIATION EXPOSURE . . . . .                           | 49  |
| 5.0 CONCLUSIONS . . . . .                                  | 51  |
| 6.0 RECOMMENDATIONS . . . . .                              | 55  |
| 7.0 REFERENCES . . . . .                                   | 57  |

CONTENTS (continued)

|                                                                                            |    |
|--------------------------------------------------------------------------------------------|----|
| APPENDIX A: Glossary of Terms . . . . .                                                    | A1 |
| APPENDIX B: List of Detection Equipment . . . . .                                          | B1 |
| APPENDIX C: Sample Calculation of Attenuation, Visibility and<br>Figure of Merit . . . . . | C1 |
| APPENDIX D: Millimeter Wave Imaging Theory . . . . .                                       | D1 |

## FIGURES

|    |                                                                                                                    |    |
|----|--------------------------------------------------------------------------------------------------------------------|----|
| 1  | Test Chamber . . . . .                                                                                             | 12 |
| 2  | Test System Schematic . . . . .                                                                                    | 13 |
| 3  | Single Section View of Test Chamber . . . . .                                                                      | 14 |
| 4  | Sketch of Method to Join Sections . . . . .                                                                        | 15 |
| 5  | Impedance vs. Moisture Content of Various Salts and Waste Tank<br>Simulants . . . . .                              | 17 |
| 6  | Conductivity of a Solution as a Function of the Salt Concentration<br>with the Target at 80 Feet . . . . .         | 18 |
| 7  | Comparison of Images Produced by Various Optical Techniques<br>with the Target at 80 Feet . . . . .                | 21 |
| 8  | Effect of Target Temperature on Visibility Through the Fog with<br>2-5 Micron Infrared Detector . . . . .          | 28 |
| 9  | Effect of Target Temperature on Visibility Through the Fog with<br>3-5 Micron Infrared Detector . . . . .          | 29 |
| 10 | Effect of Target Temperature on Visibility Through the Fog with<br>8-12 Micron Infrared Detector . . . . .         | 30 |
| 11 | Effect of Contrast Enhancement on Visible Image at 40 Feet . . . . .                                               | 33 |
| 12 | Effect of Contrast Enhancement on Visible Image at 80 Feet . . . . .                                               | 33 |
| 13 | Front End Electronics for Millimeter Wave Technique . . . . .                                                      | 40 |
| 14 | Comparison of Loss Tangent of Deionized and Salt Water . . . . .                                                   | 41 |
| 15 | Frequency Response from Trihedral Reflector in Test Chamber Filled with<br>25-Micron Diameter Salt Water . . . . . | 41 |
| 16 | Experimental Set-Up of Millimeter Wave Imaging System . . . . .                                                    | 43 |

FIGURES (continued)

|    |                                                                                          |    |
|----|------------------------------------------------------------------------------------------|----|
| 17 | Experimental W-Band System Configuration . . . . .                                       | 43 |
| 18 | Millimeter Wave Imaging of 1.5 inches Diameter Metallized Spheres .                      | 46 |
| 19 | Millimeter Wave Imaging of Various Test Targets . . . . .                                | 46 |
| 20 | Millimeter Wave Imaging of Duct Putty in Wading Pool . . . . .                           | 47 |
| 21 | Conceptual Design of Millimeter Wave Imaging System for<br>Sluicing Operations . . . . . | 47 |
| A1 | Active Illumination . . . . .                                                            | A2 |
| A2 | Backlighting . . . . .                                                                   | A2 |
| A3 | Frontlighting . . . . .                                                                  | A3 |
| A4 | Passive Emission . . . . .                                                               | A3 |
| D1 | Synthetic Aperture Data Collection Configuration . . . . .                               | D1 |

TABLES

|   |                                                                                                                                    |    |
|---|------------------------------------------------------------------------------------------------------------------------------------|----|
| 1 | Particle Size vs Type of Fog/Water Droplet . . . . .                                                                               | 11 |
| 2 | Optical Tests with 25 Micron Water Droplets (Fog) . . . . .                                                                        | 23 |
| 3 | Optical Tests with 700 Micron Water Droplets . . . . .                                                                             | 23 |
| 4 | Optical Tests with 1100 Micron Water Droplets . . . . .                                                                            | 23 |
| 5 | Optical Tests with Near Infrared Sensor . . . . .                                                                                  | 25 |
| 6 | Effect of Target Temperature on Visibility Through the Fog with<br>Infrared Detectors and 25 Micron (Fog) Water Droplets . . . . . | 26 |

TABLES (continued)

|    |                                                                                                                             |    |
|----|-----------------------------------------------------------------------------------------------------------------------------|----|
| 7  | Effect of Target Temperature on Visibility Through the Fog with Infrared Detectors and 700 Micron Water Droplets . . . . .  | 27 |
| 8  | Effect of Target Temperature on Visibility Through the Fog with Infrared Detectors and 1100 Micron Water Droplets . . . . . | 27 |
| 9  | Effect of Contrast Enhancement with Target at 40 Feet . . . . .                                                             | 32 |
| 10 | Effect of Contrast Enhancement with Target at 80 Feet . . . . .                                                             | 32 |
| 11 | Comparison of the Effect of Adding Salt to Fog/Water Droplets at 40 Feet Target Distance . . . . .                          | 35 |
| 12 | Comparison of the Effect of Adding Salt to Water Droplets at 80 Feet Target Distance . . . . .                              | 35 |
| 13 | Results of Millimeter Wave Attenuation Measurements at 94 GHz . . .                                                         | 42 |
| 14 | Millimeter Wave Imaging System Specifications . . . . .                                                                     | 48 |
| 15 | Comparison of Sensitivity of CCD and CID Cameras . . . . .                                                                  | 50 |
| 16 | Comparison of Test Results with Different Sensors . . . . .                                                                 | 52 |

## 1.0 BACKGROUND

Waste remediators have identified that surveillance of waste remediation operations and periodic inspections of stored waste are required under very demanding and difficult viewing environments. In many cases, obscurants such as dust or water vapor are generated as part of the remediation activity. Methods are required for viewing or imaging beyond the normal visual spectrum. Work space images guide the movement of remediation equipment, creating a need for rapidly updated, near real-time imaging capability. In addition, there is a need for three-dimensional topographical data to determine the contours of the wastes, to plan retrieval campaigns, and to provide a three-dimensional map of a robot's work space as basis for collision avoidance. At present, because of the closed environment in which the remediation effort is conducted, a substantial amount of time is needed to clear the atmosphere so that the effect of a remediation effort can be determined. During this time, labor costs continue and equipment is being exposed to the hazardous environment. In addition, the safety of the operation could be jeopardized because of the lack of viewing the remediation operation in near real-time.

Three methods for high-resolution, three-dimensional imaging, based upon radar, acoustic, and optical imaging techniques, have been successfully utilized in other applications. These methods require proof-of-principle testing to assure compatibility with actual environmental conditions, including electrical conductivity and density of the obscurants.

Millimeter wave (30-300 GHz) imaging systems are a likely candidate for imaging in waste tanks filled with fog. Millimeter wave imaging is effective in fog since its energy is relatively immune to the effects of water vapor in frequency "windows" of 35, 94, and 140 GHz. Water droplets in fog and clouds are considerably smaller than the wavelengths of millimeter wave signals. On the other hand, water droplets in rain are comparable in size to millimeter wavelengths, making millimeter wave imaging somewhat ineffective in rain.

Over the viewing ranges normally encountered in waste remediation activities (up to 75 feet), radar would be expected to provide image resolution and accuracy on the order of a few inches. A scanning antenna set

would be required that would cover the area to be viewed. The scan might be rotary or linear, depending on physical access to the work space and the work space configuration.

Two fundamental issues regarding any radar technique were addressed as part of this project. The first issue is electrical conductivity of the obscurant. High electrical conductivity of the medium would cause radar signal attenuation and loss of value of the method. Testing of the radar with representative obscurants is a necessity. For instance, high salt content of airborne droplets could be a significant attenuator.

The second issue is production of a robust and mechanically simple scanning antenna for this application.

An acoustic sensor is a device that sends out an acoustic pulse and tracks the time it takes for this energy to be reflected back to the sensor. Acoustic sensors generally operate in the 10-500 kHz range. Because the propagation velocity in the air is known, the time it takes to receive the reflected energy is proportional to the distance to the object reflecting the beam. One problem with this scheme is that the propagation velocity in air is a function of the temperature of the air, and it increases about 7% between 32°F and 100°F (0°C and 40°C). Many acoustic sensors have a built-in temperature compensating circuitry. Absorption of sound increases with increasing humidity and, therefore, the maximum measurement distance is reduced. The roughness, the inclination, and the size of the target surface will affect the sensing range and accuracy of the sensor. An acoustic sensor is smaller and less expensive than a radar unit. The diameter of the beam pattern on the surface that is to be measured is smaller for an acoustic beam than for a radar beam. This means that these sensors may be able to resolve smaller objects.

A video system is probably the least expensive and would require the least amount of technical development to meet the viewing needs for the sluicing operation. The equipment is available off-the-shelf. It is recognized that unmodified video imaging would not be able to view through a foggy sluicing operation. However, there are several potential methods that could be used to successfully obtain a good view of the sluicing operation.

For example, placing the lights in one riser near the area undergoing the sluicing operation and viewing the scene with a radiation-hardened camera placed down another riser away from the sluicing operation probably would greatly enhance the image. Backscatter from the fog would be eliminated. This method is called frontlighting (see "Glossary of Terms" in Appendix A). Video cameras operating with a photoconductive detector can detect energy beyond the visible wavelength region into the near-infrared region (0.8-2.2 microns). The longer the wavelength, the less scatter from the fog. The image of the scene might be less affected by the fog if the light source and/or the camera have a filter in front of them so that only near-infrared energy is used to view the scene. The filters could be made from radiation-hardened glass or quartz.

Infrared imagers in the 3-5 micron and 8-12 micron wavelength region that are commercially available could be used to view the sluicing operation. These two wavelength regions are common because they are the wavelengths where the least amount of attenuation occurs due to water vapor in the air. The output from these imagers is similar to that seen by a video camera, except that one is viewing the infrared energy from the source rather than the visible energy. Infrared imagers are a possible method for this application because less scatter occurs from the fog at longer wavelengths. The disadvantage of this approach is that the detectors need to be cooled. Infrared imagers generally are much more expensive than video cameras.

There are two approaches that can be used with infrared imagers. One approach is passive emission, in which the contents of the waste tanks are the source of the detected energy (see "Glossary of Terms" in Appendix A). Infrared imagers can measure temperature differences of a few degrees Fahrenheit. This would eliminate backscatter from the light source to the detector (i.e., it would be like the frontlighting technique discussed above) which would further enhance the viewing of the scene. However, there must be some contrast (a difference in temperature or emissivity) between the object to be viewed and the surroundings in order to detect an object. It is doubtful that sufficient contrast would exist in a waste tank to allow the use of passive emission.

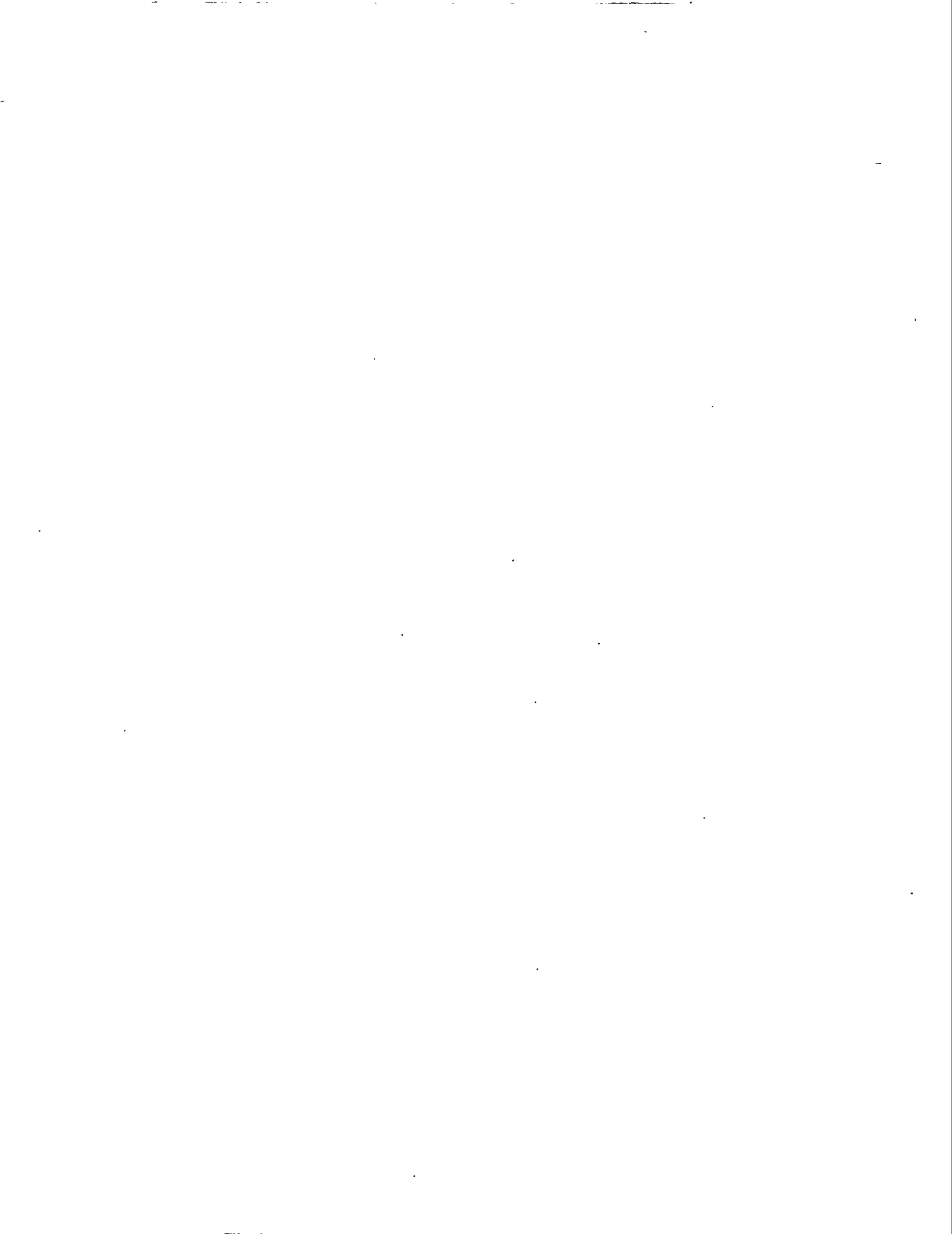
The other approach is active illumination, in which an external source of infrared energy is used to illuminate the scene (see "Glossary of Terms" in Appendix A). The active illumination could be backlighted (less scatter from the fog will occur because of the longer wavelength), frontlighted, or backlighted with a selective ventilation system which would blow the fog away from the light source.

Finally, laser range finding is another approach for obtaining an image during the sluicing operation. Present-day commercially available laser range finders raster a pulsed laser beam over the viewing area using articulated mirrors. Present state-of-the-art are amplitude-modulated range finders that measure phase angle shift of reflected light to produce range data and display this data in a color-coded imager. Range data is produced by commercially available laser range finders in digital form that can be readily accepted by a robot controller or a visual imaging system. According to manufacturers' literature, resolution and accuracy on the order of 0.5 inch over a range of 75 feet can be achieved with a laser range finder.

Range finders predicated on lasers are subject to signal attenuation and refraction/reflection by obscurants. Signal attenuation due to absorption by water vapor can be overcome by tuning the laser wavelength outside of the absorption bands for water. This has been successfully accomplished for military applications, such as target designators and gunnery range finders. These devices are also effective in man-produced obscurants, such as smokes. Large water droplets suspended in air could cause significant reflection and refraction that would produce range errors. As a result, effects of the actual obscurant, be it condensed water vapor, suspended water droplets or dust, must be specifically evaluated before a firm value prediction of this method for the intended application can be provided.

Specialized software has been developed to manipulate range data with such features as user-selectable viewing perspective, noise and error rejection, and a limited autonomous image interpretation feature.

In all of these methods, it will be necessary to keep the entrance window of the camera system clean and warm to prevent condensation from forming. Video image processing could be used with any of these techniques to enhance the image in real-time or near real-time.



## 2.0 REVIEW OF CANDIDATE METHODS

The waste tank remediation work being conducted at the Hanford site was used as a model for the requirements of a viewing system. A meeting was held with Westinghouse Hanford Corporation (WHC) personnel, and the following requirements were suggested for a system for viewing through obscurants during a sluicing operation:

1. The system should provide a real-time or near real-time (5-minute update time) image of waste surface.
2. The system should produce an image equivalent to a closed circuit television (CCTV) system image. The image would preferably be in color, with the same level of depth discrimination as in a CCTV image.
3. The system should provide capability for storing and retrieving images.
4. The system must be able to view the entire waste surface with a minimum field-of-view of 20°. It is desirable to be able to image the entire tank interior.
5. The imaging system must be capable of indicating relative position of view within the tank.
6. The system must be able to be placed through a 12" riser.
7. The waste tank is 75 feet in diameter.
8. The imaging system must be able to view through sluicing fog.
  - Nozzle/stream atomization
  - Condensation/evaporation
  - Splash effects
9. The system must be designed to be readily decontaminated.
  - Glove box may be required.
  - Decontamination chemicals must be compatible with tank operating requirement.
10. The desired operational life for the system is two years.
11. The system must be compatible with 100 R/hr at the dome radiation field in-tank.

12. The system must be capable of discriminating objects down to 12 inches in size at a range of 75 feet. A size discrimination of two inches would be desirable.
13. If system maintenance access frequency is 30 days or greater, the system installation can be hands on. If system maintenance access frequency is less than 30 days, the system must be self deploying.
14. The following are tank environmental conditions:
  - Nitrate-based caustic (airborne)
  - 100% relative humidity at between 60<sup>o</sup> to 140<sup>o</sup> F
  - Unknown organics (relatively non-volatile)
  - Airborne waste particulates.
15. System output displays shall be remotely located in the sluicing control room (approximately 500 feet).
16. Control room components must be compatible with trailer temperature.
17. System failures, which would preclude removal of the equipment from the tank, are unacceptable.
18. External environmental conditions must be compatible with standard Hanford weather conditions, including solar heating and blowing dust.
19. A maintenance frequency goal is to require no maintenance during a 6-month period of operations.
  - If monthly maintenance is required, then it must be able to be accomplished in one shift.
  - If maintenance frequency is six months, then a maintenance outage may be up to one week.

A brainstorming session was held with WHC and PNL staff. Various methods were discussed, including the following:

1. Infrared sensors/cameras (3-5 micron and 8-12 micron).
  - passive emission
  - active illumination

## 2. Conventional video imaging

- with backlighting.
- with frontlighting.
- with infrared filters for near-infrared viewing.

3. Duplex system: Moving the camera/sensor up close to minimize range in obscurant, then assembling multiple views into a single image with digital image processing. Several commercially available software packages available.

4. Millimeter wave (90 GHz) Synthetic Aperture imaging.

5. Laser range finding.

6. Pulsed laser gating.

7. Acoustics.

Pulsed laser gating has been successfully used in underwater imaging. A pulsed laser is used to illuminate the target at certain time intervals; backscatter is reduced by range gating, whereby the detector is gated to cut out the backscatter produced by the outgoing pulse and detects only the return pulse. Range gating does not eliminate the influence of scatter or other inhomogeneities on the return light, but the detector is less susceptible to ambient light. No commercial pulse laser gating system is available off the shelf, and development work would be required to adapt a system for waste tank applications. For example, for the short distance being used in the waste tank, electronics that operate with nanosecond time delays would be required. Discussions were held with Science Applications International Corporation (SAIC) in San Diego, CA, on adapting a laser range gating system that they have developed for underwater applications for the short target distances needed for waste tank applications. It was not possible within the funding level and time frame of this program to pursue this approach.

In addition to the methods discussed in the brainstorming session, several other methods were considered in the course of this program. For example, work has recently been declassified on methods to burn holes through clouds using a CO<sub>2</sub> laser. This may have application for waste tank applications; however, this is a developmental idea and there is no system commercially available that can perform this task.

The other methods that were suggested in the brainstorming session are feasible candidates for viewing through obscurants and were tested as part of this study. Most of these have already been described in the Background section of this report. PNL is unique in having equipment available that could be used to evaluate and test these various methods.

### 3.0 TEST RESULTS

#### 3.1 TEST SET-UP

The test chamber that was used to test the various methods for imaging through obscurants is shown in Figure 1, while Figures 2 and 3 show the components of the test chamber. The chamber consisted of four sections of fiberglass tube, each three feet in diameter and ten feet long. The adjacent tube sections were attached to each other using a rubber clamp and a sheet metal clamp, as shown in Figure 4. Thus, the test chamber was 40 feet long with open ends so that the instruments and target could be mounted without getting wet. A pump and air compressor fed water and air through piping at the top of the test chamber to spray nozzles in the chamber. The test chamber was mounted on wooden supports to bring the fixture to working level. Three sets of changeable nozzles were used for these tests: one set of nozzles produced 25-micron size particles (fog) at a flow rate of 0.05 gallons/minute, a second set of nozzles produced 700-micron size particles (water droplets) at a flow rate of 0.5 gallons/minute, and a third set of nozzles produced 1100-micron size particles (at a flow rate of 1.7 gallons/minute).

The size of the water particles was determined by using information supplied by the manufacturer of the nozzles (Spraying Systems Co., Wheaton, IL). The particle size was based on the water and/or air pressure supplied by the system. Table 1 lists mean particle size for different types of fog/water droplets (Spraying Systems Co. 1981). The water collected in the chamber was funneled through hoses to a holding tank (16-gallon wash basin), then recirculated through the system.

TABLE 1. Particle Size vs. Type of Fog/Water Droplets

| Particle Size Range<br>Median Volume<br>(microns) | Comparative<br>Subject |
|---------------------------------------------------|------------------------|
| Below 0.001                                       | Molecular Dimensions   |
| 0.001-0.01                                        | Smoke                  |
| 0.01-1.0                                          | Fumes                  |
| 2-10                                              | Dry Fog                |
| 10-50                                             | Wet Fog                |
| 50-100                                            | Misty Rain             |
| 100-500                                           | Light Rain             |
| 500-1000                                          | Moderate Rain          |
| 1000-2000                                         | Intense Rain           |
| 2000-5000                                         | Heavy Rain             |



FIGURE 1. Test Chamber

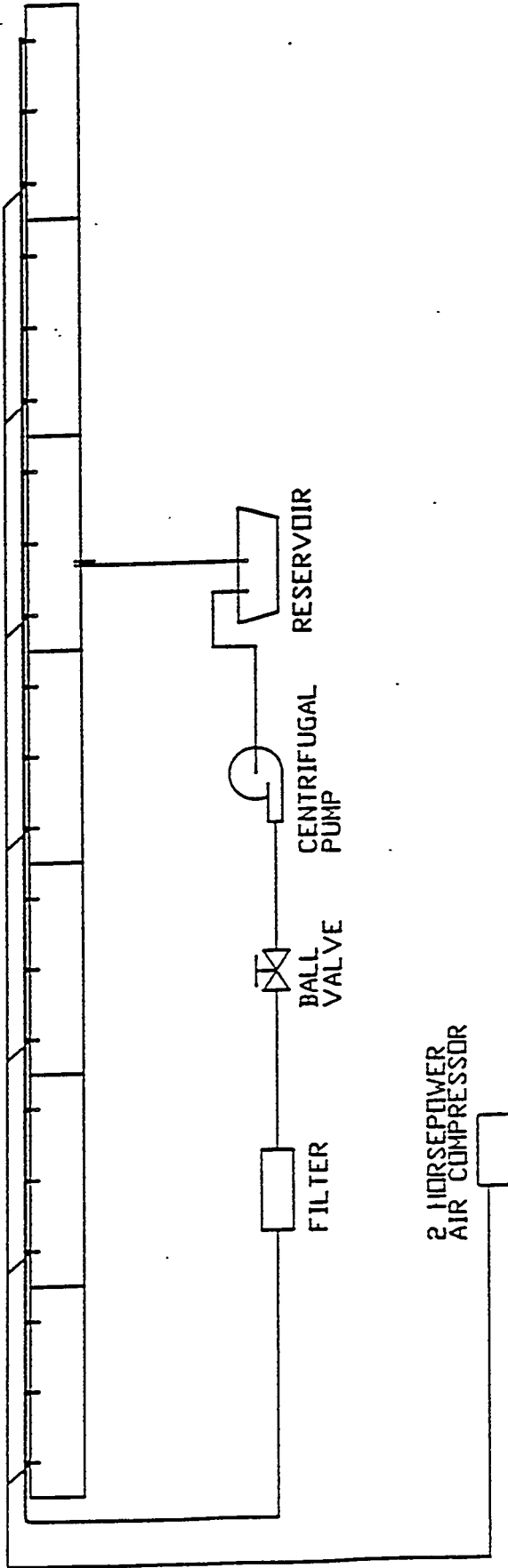
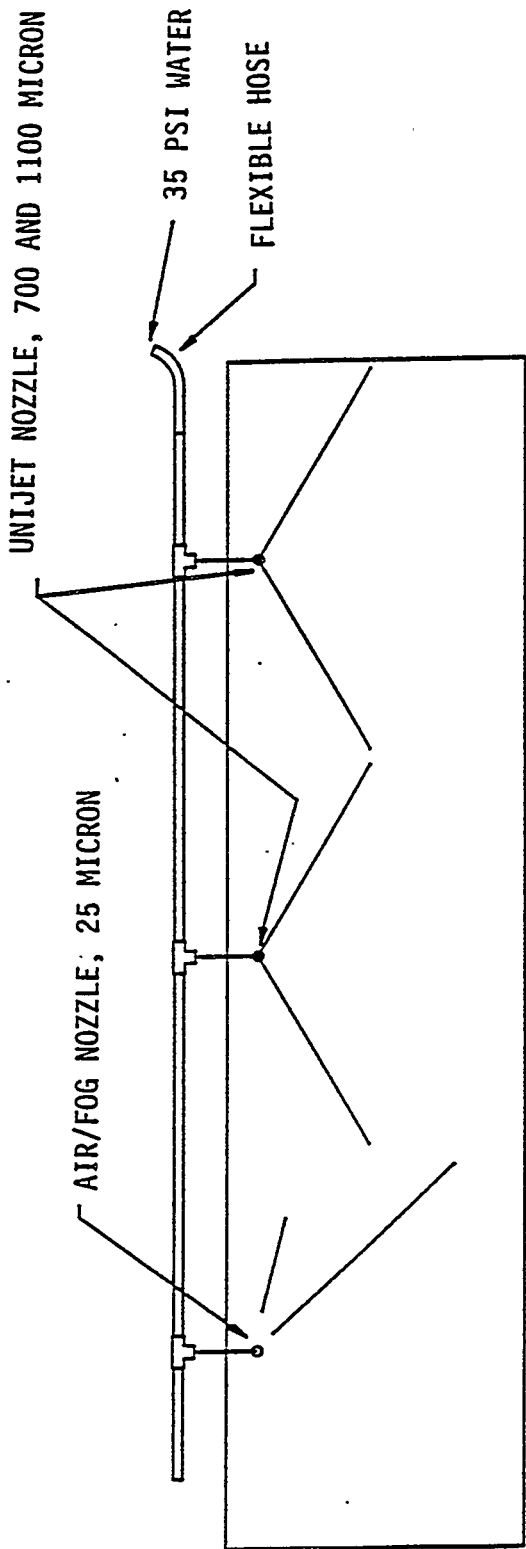


FIGURE 2. Test System Schematic



**FIGURE 3.** Single Section View of Test Chamber

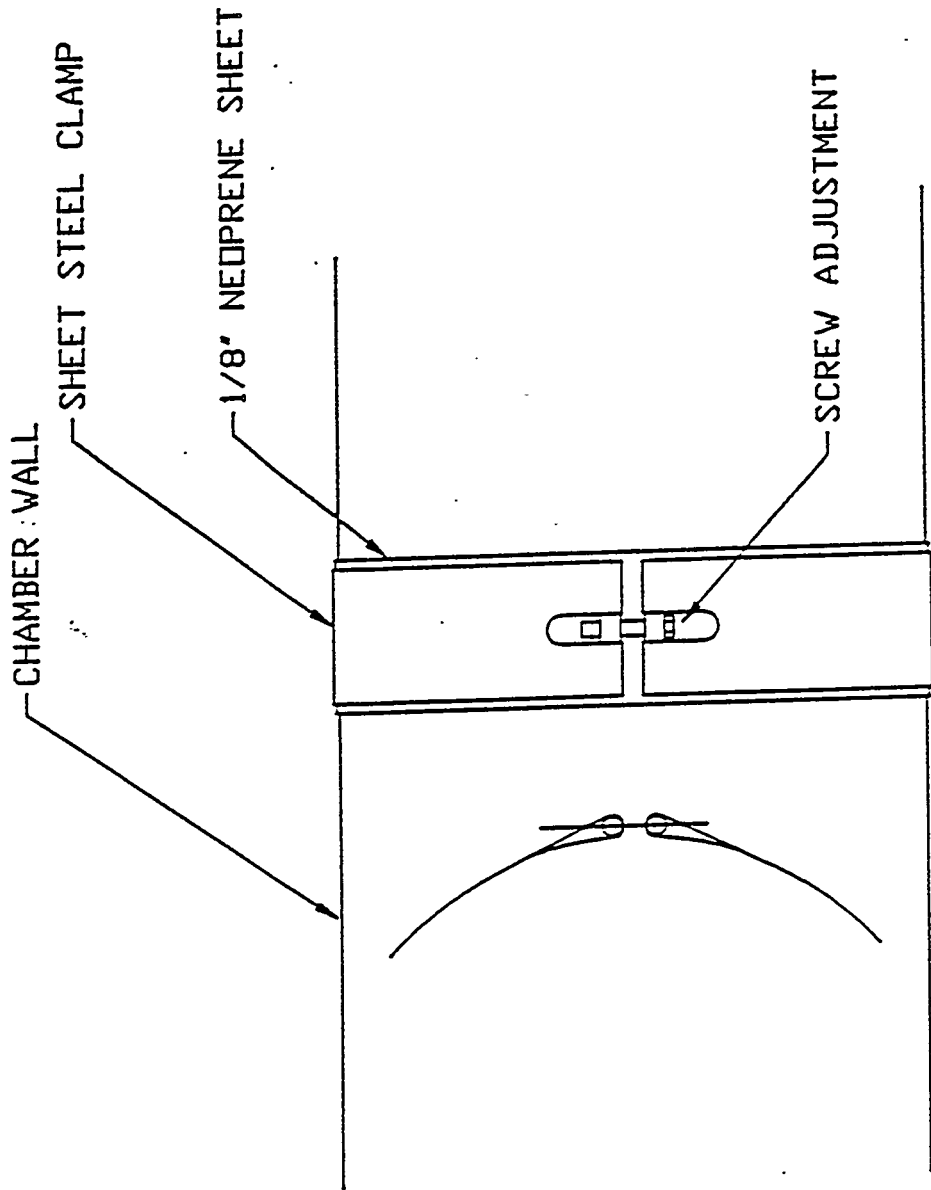


FIGURE 4. Sketch of Method to Join Sections

Initial tests were conducted with no water in the chamber, in order to get a baseline measurement. Next, water with no salt in it was circulated through the system using the three different nozzles. Finally, salt was added to the water in the holding tank in concentrations up to 20% by weight and circulated through the chamber. The salt used in this test was rock salt (sodium chloride), similar to that used in water softeners. Testing conducted at PNL using simulated tank waste chemicals indicated that the conductivity of the simulants could be simulated using ordinary sodium chloride, as shown in Figure 5 (Hockey 1993). Testing also indicated that a salt concentration of approximately 20% produced a peak conductivity. This is consistent with the data from the Handbook of Chemistry and Physics (Weast 1976-1977, p. D-269) and plotted in Figure 6 with some experimental data. The addition of higher concentrations of salt resulted in not all of the salt being dissolved and a scum appearing on the surface of the water tank.

Measurements were made, first with a target-detector separation of 40 feet, and then a front-surface aluminized mirror was used to increase the path length to 80 feet (double pass through the 40-foot long test chamber). Tests were conducted by placing a target on the open ends of the fiberglass tube. Target properties were selected to meet requirements for the different instruments to be tested. For the optical tests, the target was an oxidized steel plate whose diffuse reflectivity was measured to be 25%. For the infrared test, the target was a blackbody source with a emissivity of 1.0 and whose temperature was varied from 5°F to 50°F above ambient. For the acoustic tests, the target was a flat piece of metal which would reflect 100% of the expanding acoustic beam from the sensor. The millimeter wave system measured the attenuation through the test chamber, and its target was a trihedral (corner cube reflector) that was a 100% specular reflector. In addition, imaging tests were conducted with the millimeter wave systems using a variety of targets. A list of the detectors used for these tests is given in Appendix B.

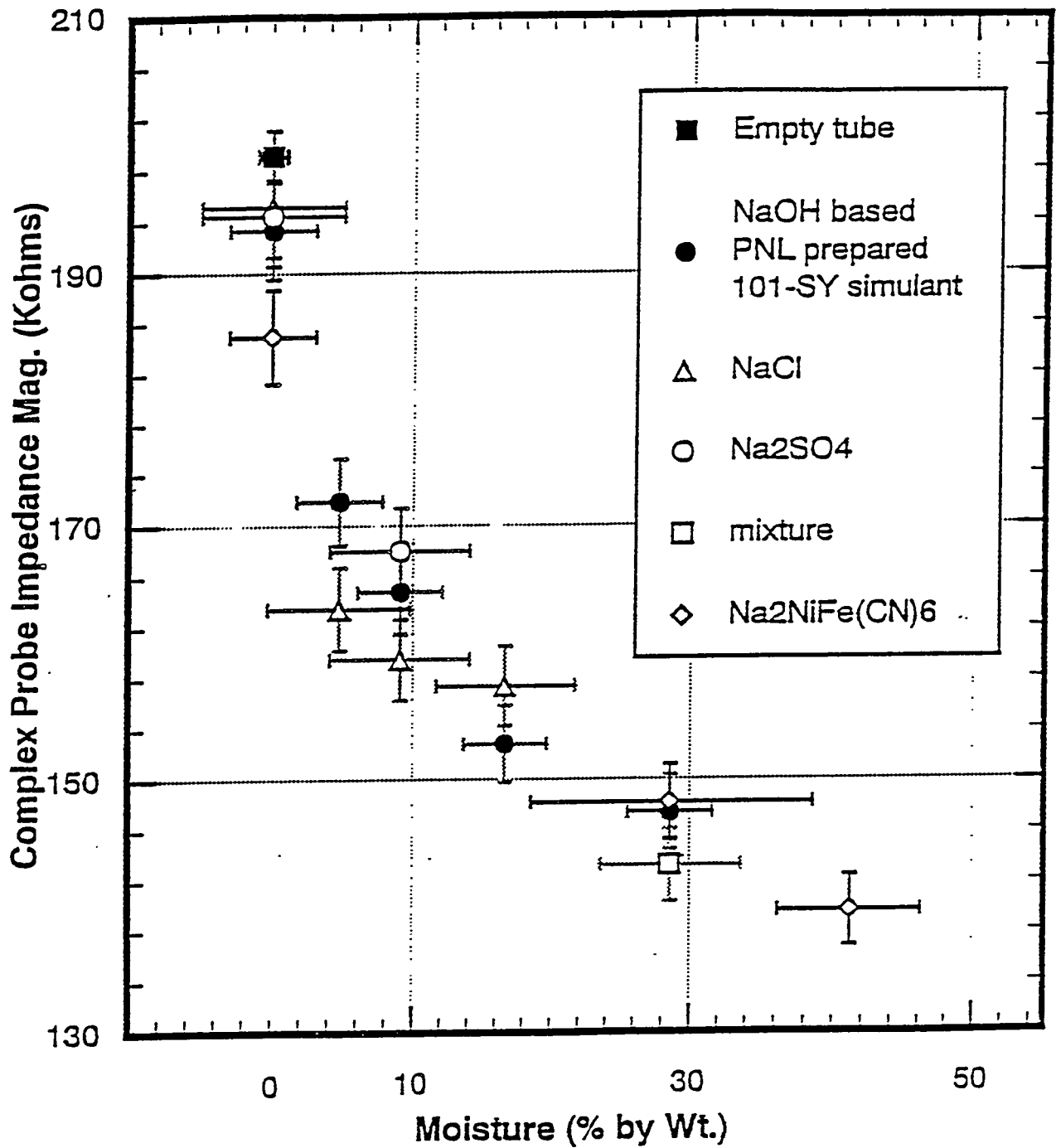


FIGURE 5: Impedance vs. Moisture Content of Various Salts and Waste Tank Simulants (Hockey 1993)

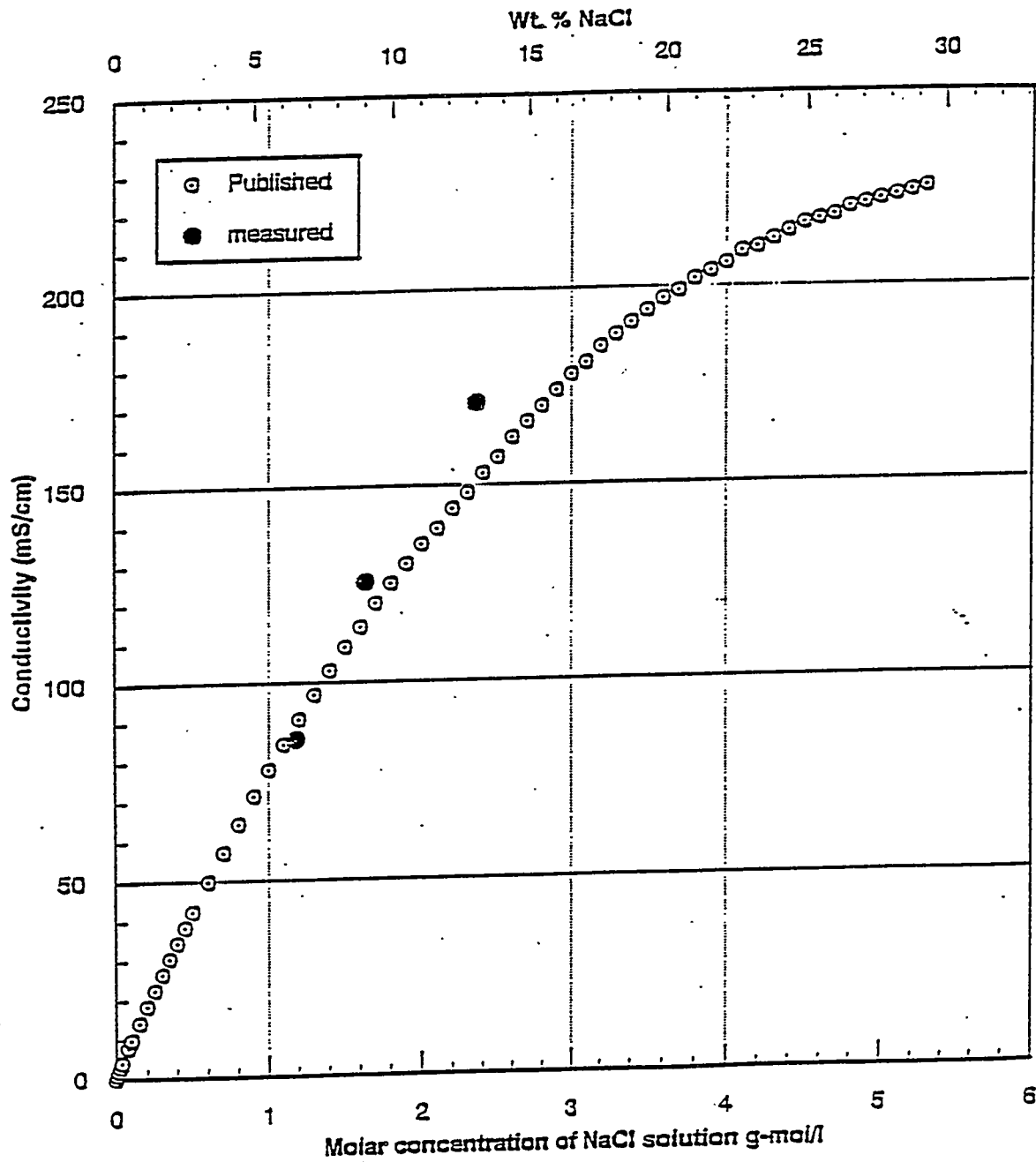


FIGURE 6: Conductivity of a Solution as a Function of Salt Concentration

## 3.2 DISCUSSION OF TESTS

### 3.2.1 Optical Sensors

The sensors chosen for this test are listed in Appendix B. The visible charge coupled device (CCD) camera, which had a silicon detector that operates in the 0.4-1.1 micron wavelength region, was chosen because of its small size (the head is 1.5 x 1.5 x 2 inches), high sensitivity, and its controller allowed a wide variation of the operating parameters (gain, gamma, gray scale, etc). A charge injection device (CID) camera, which operates in the same wavelength region as the CCD device but is reported to have better radiation tolerance, was also tested. A video camera with a photoconductive detector which operates in the 0.4-2.2 micron wavelength region was used to determine if backscatter could be minimized by viewing the target in the near-infrared. The 3.2-5.6 micron infrared camera was used because it was an infrared camera that does not require liquid nitrogen cooling and had been placed in waste tanks on the Hanford site. To determine the effect of liquid nitrogen cooling on the sensitivity of the detector, an AGA Thermovision system that operates in the 2.0-5.6 micron wavelength range was also used in these tests. The 8-12 micron infrared camera also required liquid nitrogen cooling. The instruments used in these tests were chosen because they were readily available from sources on the Hanford site, and the use of the instruments listed in Appendix B does not imply an endorsement of these products.

The test chamber could effectively be filled with fog or water droplets. With only the fog nozzles operating (one nozzle for each ten-foot section), the chamber could be filled up with fog of a density such that a 500-watt tungsten lamp (irradiance measured at 13.5 mw/cm<sup>2</sup> when approximately two feet from the lamp) could not be seen through 40 feet of the chamber. Visibility was determined to be about 15 feet when the chamber was filled with fog. Visibility through the water droplets with all of the nozzles operating was calculated to be 60 feet for the 700-micron water droplets and 80 feet with the 1100-micron water droplets using the oxidized steel plate target illuminated by room lights (illumination measured to be 408 lux, or 38 ft-c).

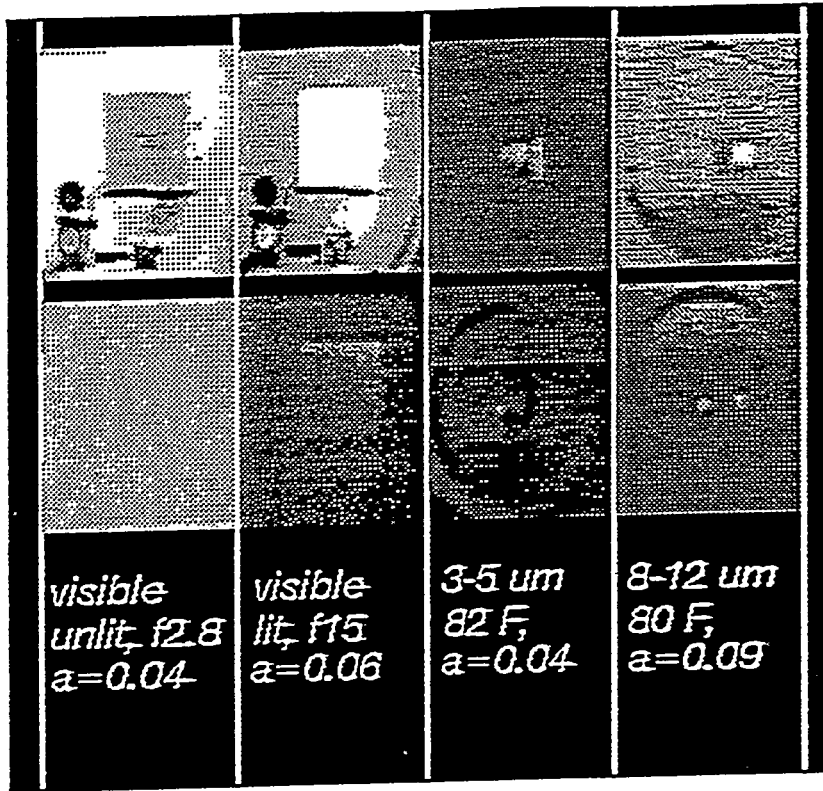
It was not possible to view with the optical systems through 40 feet of fog as dense as could be produced in the test chamber. For the tests with the fog nozzles, the procedure was to fill the chamber with fog, then turn the system off (except for a low air flow through the nozzles in order to keep the fog uniform). The fog density decreased with time after the waterflow was stopped. When the object first became visible to the detector, the transmission of a helium-neon laser beam (0.6328 microns) sent through the 40-foot path length was measured. The attenuation of the fog is given by the equation:

$$T = \exp(-ax) \quad (1)$$

where  $T$  = Transmission of the laser beam  
 $a$  = attenuation of the fog or water droplets ( $\text{feet}^{-1}$ )  
 $x$  = distance (40 feet)

By measuring the transmission of the helium-neon laser beam through the fog/water droplets when the oxidized steel plate was just barely visible, it is possible to convert the calculated attenuation into a number that describes the visual range of the object, i.e., the visibility through the fog or water droplets (see "Glossary of Terms" in Appendix A). This is done by re-applying equation 1 (Block 1993), and an example calculation is shown in Appendix C. Figure 7 compares the images produced by several optical techniques when the target was barely visible.

The test results that are tabulated are stated in both the attenuation of the fog/water droplets and the visibility through the fog/water droplets. Both of these are measured at 0.63 microns when the target is just barely visible at 40 or 80 feet using the stated detection/illumination method. The size of the fog/water droplets was much greater than the wavelength of visible light; therefore, there would not be a significant difference between the scattering at the helium-neon laser wavelength (0.63 microns) and the rest of the visible spectrum. The more the air cleared in the test chamber, the higher the measured transmission of the laser beam, the smaller the attenuation of the fog will be, and the longer the visibility range will be. If the target is at 40 feet and the visibility of the fog/water droplets is



Top Images are with No Fog in the Test Chamber  
 Bottom Images are with 25 Micron Fog in the Test Chamber  
 a = Absorption ( $\text{ft}^{-1}$ ) Target Emissivity = 0.75  
 Target Size: 7.5 x 7.5 in.

FIGURE 7: Comparison of Images Produced by Various Optical Techniques  
 with the Target at 80 Feet

30 feet, then the target could be detected by the sensor, even though it could not be seen visibly. If the target is at 40 feet and the visibility of the fog/water droplets is 60 feet, then the target could not be detected by the sensor until it could be easily seen with the naked eye because there is a large amount of scatter and absorption from the fog/water droplets with this detection scheme. Also stated in the results tables is a "figure of merit", which is the ratio of the target distance to the visibility of the fog/water droplets (see "Glossary of Terms" in Appendix A). A "figure of merit" of unity means that the stated detection/illumination scheme was able to detect the target (an oxidized steel plate illuminated by room lights, 38 ft-c) at the target distance. The larger the figure of merit, the better the detection/illumination scheme is for imaging through fog/water droplets.

### Test Results

The results of the tests with fog and water droplets without salt added to the mixture are summarized in Tables 2 through 4. In backlighting, the 500-watt light source is placed near the detector, and its light is projected down the test chamber to the target by the detector (see "Glossary of Terms" in Appendix A). With the fog in the chamber, the amount of light from the tungsten lamp that reflected from the fog was measured to be approximately 3.8%. Backlighting could not be done at 80 feet because the test chamber was only 40 feet long and it was not possible to separate at the target plane the backscattered light from the light that went through the fog/water droplets. Two levels of frontlighting were tested (see "Glossary of Terms" in Appendix A). In one case, the room lights were used, which produced an irradiance of about  $17 \mu\text{W}/\text{cm}^2$  on the target plane; in the other case, a 500-watt lamp was used, which produced an irradiance of about  $0.185 \text{ mW}/\text{cm}^2$  on the target plane. This would simulate two lighting schemes, one in which the light is far from the target and illuminating a large area from above the target (not along the same path) and the other in which a light is placed on a robotic arm close to that target. The lens used with the CCD camera that operated in the visible region had an F-stop of approximately f/2.8 when used with room lights only frontlighting scheme and an F-stop of f/22 when used with the 500-watt tungsten lamp as the light source.

**TABLE 2. Optical Tests with 25-Micron (Fog) Water Droplets**

| Wavelength Region | Target Distance    |                                     |                 |                    |                                     |                 |
|-------------------|--------------------|-------------------------------------|-----------------|--------------------|-------------------------------------|-----------------|
|                   | Attenuation* (/ft) | 40 Feet<br>Visi-<br>bility*<br>(ft) | Figure of Merit | Attenuation* (/ft) | 80 Feet<br>Visi-<br>bility*<br>(ft) | Figure of Merit |
| Visible           |                    |                                     |                 |                    |                                     |                 |
| Backlight         | 0.050              | 60                                  | 0.67            | ----               | ----                                | ----            |
| Frontlight        |                    |                                     |                 |                    |                                     |                 |
| Room Lights       | 0.076              | 40                                  | 1.00            | 0.038              | 79                                  | 1.01            |
| 500 w Bulb        | 0.102              | 30                                  | 1.33            | 0.054              | 56                                  | 1.43            |
| 2-5 Micron        | 0.088              | 34                                  | 1.18            | 0.032              | 94                                  | 0.85            |
| 3-5 Micron        | 0.059              | 51                                  | 0.78            | 0.019              | 159                                 | 0.50            |
| 8-12 Micron       | 0.107              | 28                                  | 1.42            | 0.076              | 40                                  | 2.00            |

**TABLE 3. Optical Tests with 700-Micron Water Droplets**

| Wavelength Region | Target Distance    |                                     |                 |                    |                                     |                 |
|-------------------|--------------------|-------------------------------------|-----------------|--------------------|-------------------------------------|-----------------|
|                   | Attenuation* (/ft) | 40 Feet<br>Visi-<br>bility*<br>(ft) | Figure of Merit | Attenuation* (/ft) | 80 Feet<br>Visi-<br>bility*<br>(ft) | Figure of Merit |
| Visible           |                    |                                     |                 |                    |                                     |                 |
| Backlight         | 0.099              | 68                                  | 0.59            | ----               | ----                                | ----            |
| Frontlight        |                    |                                     |                 |                    |                                     |                 |
| Room Lights       | >0.113             | <60                                 | >0.67           | 0.046              | 146                                 | 0.55            |
| 500 w Bulb        | >0.113             | <60                                 | >0.67           | 0.078              | 86                                  | 0.93            |
| 2-5 Micron        | 0.050              | 134                                 | 0.30            | 0.026              | 259                                 | 0.31            |
| 3-5 Micron        | 0.032              | 210                                 | 0.19            | 0.010              | 672                                 | 0.12            |
| 8-12 Micron       | 0.038              | 177                                 | 0.23            | 0.020              | 336                                 | 0.24            |

**TABLE 4. Optical Tests with 1100-Micron Water Droplets**

| Wavelength Region | Target Distance    |                                     |                 |                    |                                     |                 |
|-------------------|--------------------|-------------------------------------|-----------------|--------------------|-------------------------------------|-----------------|
|                   | Attenuation* (/ft) | 40 Feet<br>Visi-<br>bility*<br>(ft) | Figure of Merit | Attenuation* (/ft) | 80 Feet<br>Visi-<br>bility*<br>(ft) | Figure of Merit |
| Visible           |                    |                                     |                 |                    |                                     |                 |
| Backlight         | 0.065              | 103                                 | 0.39            | ----               | ----                                | ----            |
| Frontlight        |                    |                                     |                 |                    |                                     |                 |
| Room Lights       | >0.084             | <80                                 | 0.50            | 0.041              | 164                                 | 0.49            |
| 500 w Bulb        | >0.084             | <80                                 | 0.50            | 0.073              | 92                                  | 0.87            |
| 2-5 Micron        | 0.050              | 134                                 | 0.29            | 0.018              | 374                                 | 0.21            |
| 3-5 Micron        | 0.040              | 168                                 | 0.24            | 0.006              | 1121                                | 0.07            |
| 8-12 Micron       | 0.024              | 280                                 | 0.14            | 0.013              | 517                                 | 0.15            |

\* Attenuation and Visibility measured at 0.63 Microns

The spectral response of the silicon detector in the CCD camera was not high beyond 0.8 microns. As a result, it was not possible to view the target in the near-infrared (0.8-2.5 microns) with this camera. However, a camera with a photoconductive sensor that operated in the visible and near-infrared wavelength region (0.4-2.2 microns) was used to determine if the backscatter from the fog/water droplets could be minimized by placing a long pass infrared filter in front of the camera and using a 100-watt mercury arc lamp to backlight the target. The output of the lamp was measured to be 20 mw/cm<sup>2</sup> two feet from the lamp and 0.07 mw/cm<sup>2</sup> on the target plane 40 feet from the lamp. The results, summarized in Table 5, indicate that there was no appreciable gain in operating in the near-infrared wavelength region. Less backscatter was observed from the fog/water droplets when a 0.85 micron long pass filter was placed in front of the camera; however, the amount of energy reaching the detector decreased because the energy reflected from the target in the visible wavelength region was eliminated by the filter. Testing with this type of camera was difficult because the image took several seconds to clear from the sensor (image persistence). This would make this type of camera difficult to use for waste tank applications.

The results of the tests indicate that optical techniques could not be used to view through a dense fog/water droplets. In the visible region, except when the target is frontlighted, the visibility of the fog/water droplets needs to be at least equal to the distance to the target in order to view the target. Objects can be detected in 50%-100% thicker fog and 15%-30% thicker water droplets using frontlighting compared to using backlighting. The higher the fog/water droplet density, the greater the degradation of the image due to backlighting. The more intense the light source, the greater gain from frontlighting.

With fog in the chamber, use of an image intensified camera was attempted. The results indicate that there was no appreciable gain in the visibility of the target by using an intensified camera in comparison to a CCD camera. Reflections caused sections of the image to bloom while other sections were not even visible until the fog cleared. In addition, the laser used to determine the transmission of the fog caused blooming in the camera and could not be used with the intensified camera.

TABLE 5. Optical Tests with Near-Infrared Sensor

| Wavelength Region       | Attenuation* (/ft) |       | Target Distance   |    | Figure of Merit |      |
|-------------------------|--------------------|-------|-------------------|----|-----------------|------|
|                         |                    |       | 40 Feet           |    |                 |      |
| Particle Size (Microns) | 25                 | 700   | Visi-bility* (ft) |    | 25              | 700  |
|                         | Visible            | 0.042 | 0.085             | 72 | 79              | 0.56 |
| Near-Infrared           | 0.044              | 0.085 | 68                | 79 | 0.59            | 0.51 |

\* Attenuation and Visibility measured at 0.63 microns

The operation of a laser range finder was tested in the fog/water droplet chamber. The range finder operated in the near-infrared wavelength region (0.83 microns). It was able to scan the target area at 40 feet in a few seconds. The results indicate that the backscatter from the fog/water droplets resulted in the range finder losing its ability to determine the range to a target. However, images were obtained through a fog which had a transmission of 11% (attenuation of 0.055/foot, visibility of 55 feet). The image produced by the range finder for a target at 40 feet was equivalent to a video image produced with the target at 80 feet.

For a water droplet spray, the ability of the range finder to image a target was dependent on the proximity of the laser range finder to the nozzles. With the target (aluminum foil with a reflectance of approximately 80%) and all of the nozzles set at the far end of the tube, the range finder was able to image up to a transmission of 10.5% (attenuation of 0.056/foot, visibility of 120 feet) for the 700-micron water droplets and 13.7% (attenuation of 0.050/foot, visibility of 134 feet) for the 1100-micron water droplets. However, if the nozzles were placed within 16 feet of the laser range finder, then the range finder could not view through even one nozzle due to backscatter from the water droplets. The images exhibited random white and black pixels. No filtering algorithm, compatible with the system's software, was available that could remove this random noise. Range information inside and beyond the water droplets was lost completely.

Infrared techniques did enhance the image through the fog, but showed a higher degradation of the image than visible techniques with the water droplets. Cryogenic cooling of the infrared detector greatly enhances the

ability of the instrument to detect a target by decreasing the noise in the detector when compared to using a thermoelectric cooler for cooling the infrared detector.

The infrared tests were conducted with the hot plate target at a temperature 5°F to 10°F above ambient. To determine the effect of temperature on the visibility through the fog/water droplets, a test was conducted in which a black-body source (emissivity=1) was set at different temperatures and the visibility through the fog was determined. The results are shown in Tables 6 through 8 and plotted in Figures 8 through 10. The results indicate that increasing the differential between the target and ambient temperatures will allow the target to be viewed in denser fog. The effect is more pronounced when there is greater scattering from the fog/water droplets.

The infrared cameras could be set with different temperature ranges, e.g., 5°F, 20°F, etc. The Inframetrics camera also had the ability of zoom-in on the target. Tests were generally conducted with the infrared cameras set at a 20°F temperature range. The zoom feature was activated because it made the image easier to detect, especially when viewed through the long tube that makes up the test chamber. There was no appreciable change in the results reported in Tables 2 through 4 when the infrared systems were set to a wider field-of-view or a lower temperature range because the contrast with the background also changed when these parameters were reset.

**TABLE 6.** Effect of Target Temperature on Visibility Through the Fog with Infrared Detectors and 25-Micron (Fog) Water Droplets

| Wavelength Region | Target Distance    |                                     |                 |                    |                                     |                 |
|-------------------|--------------------|-------------------------------------|-----------------|--------------------|-------------------------------------|-----------------|
|                   | Attenuation* (/ft) | 40 Feet<br>Visi-<br>bility*<br>(ft) | Figure of Merit | Attenuation* (/ft) | 80 Feet<br>Visi-<br>bility*<br>(ft) | Figure of Merit |
| 2-5 Micron        |                    |                                     |                 |                    |                                     |                 |
| 83°F              | 0.088              | 34                                  | 1.18            | 0.032              | 94                                  | 0.85            |
| 100°F             | 0.107              | 28                                  | 1.42            | 0.052              | 58                                  | 1.38            |
| 120°F             | 0.132              | 23                                  | 1.74            | 0.060              | 50                                  | 1.60            |
| 3-5 Micron        |                    |                                     |                 |                    |                                     |                 |
| 83°F              | 0.059              | 51                                  | 0.78            | 0.019              | 158                                 | 0.51            |
| 100°F             | 0.089              | 34                                  | 1.18            | 0.047              | 64                                  | 1.25            |
| 120°F             | 0.105              | 29                                  | 1.38            | 0.059              | 51                                  | 1.57            |
| 8-12 Micron       |                    |                                     |                 |                    |                                     |                 |
| 83°F              | 0.107              | 28                                  | 1.43            | 0.076              | 40                                  | 2.00            |
| 100°F             | 0.146              | 21                                  | 1.90            | 0.103              | 29                                  | 2.76            |
| 120°F             | 0.155              | 19                                  | 2.10            | 0.111              | 27                                  | 2.96            |

**TABLE 7.** Effect of Target Temperature on Visibility Through the Fog with Infrared Detectors and 700-Micron Water Droplets

| Wavelength Region | 40 Feet            |                  |                 | 80 Feet            |                  |                 |
|-------------------|--------------------|------------------|-----------------|--------------------|------------------|-----------------|
|                   | Attenuation* (/ft) | Visibility* (ft) | Figure of Merit | Attenuation* (/ft) | Visibility* (ft) | Figure of Merit |
| 2-5 Micron        |                    |                  |                 |                    |                  |                 |
| 83°F              | 0.050              | 134              | 0.30            | 0.026              | 259              | 0.31            |
| 100°F             | 0.085              | 79               | 0.51            | 0.050              | 134              | 0.60            |
| 120°F             | 0.113              | 60               | 0.67            | 0.056              | 120              | 0.67            |
| 3-5 Micron        |                    |                  |                 |                    |                  |                 |
| 83°F              | 0.032              | 210              | 0.19            | 0.010              | 672              | 0.12            |
| 100°F             | 0.050              | 134              | 0.30            | 0.032              | 210              | 0.38            |
| 120°F             | 0.078              | 86               | 0.46            | 0.038              | 177              | 0.45            |
| 8-12 Micron       |                    |                  |                 |                    |                  |                 |
| 83°F              | 0.038              | 177              | 0.23            | 0.020              | 336              | 0.24            |
| 100°F             | 0.056              | 120              | 0.33            | 0.038              | 177              | 0.45            |
| 120°F             | 0.085              | 79               | 0.51            | 0.043              | 156              | 0.51            |

**TABLE 8.** Effect of Target Temperature on Visibility Through the Fog with Infrared Detectors 1100-Micron Water Droplets

| Wavelength Region | 40 Feet           |                 |                 | 80 Feet           |                 |                 |
|-------------------|-------------------|-----------------|-----------------|-------------------|-----------------|-----------------|
|                   | Attenuation (/ft) | Visibility (ft) | Figure of Merit | Attenuation (/ft) | Visibility (ft) | Figure of Merit |
| 2-5 Micron        |                   |                 |                 |                   |                 |                 |
| 83°F              | 0.050             | 134             | 0.30            | 0.018             | 374             | 0.21            |
| 100°F             | 0.073             | 92              | 0.43            | 0.050             | 134             | 0.60            |
| 120°F             | 0.084             | 80              | 0.50            | 0.060             | 112             | 0.71            |
| 3-5 Micron        |                   |                 |                 |                   |                 |                 |
| 83°F              | 0.040             | 168             | 0.24            | 0.006             | 1121            | 0.07            |
| 100°F             | 0.060             | 112             | 0.36            | 0.024             | 280             | 0.28            |
| 120°F             | 0.084             | 80              | 0.50            | 0.031             | 217             | 0.37            |
| 8-12 Micron       |                   |                 |                 |                   |                 |                 |
| 83°F              | 0.024             | 280             | 0.14            | 0.013             | 517             | 0.15            |
| 100°F             | 0.040             | 168             | 0.24            | 0.024             | 280             | 0.28            |
| 120°F             | 0.065             | 103             | 0.39            | 0.031             | 217             | 0.37            |

\* Attenuation and Visibility measured at 0.63 microns

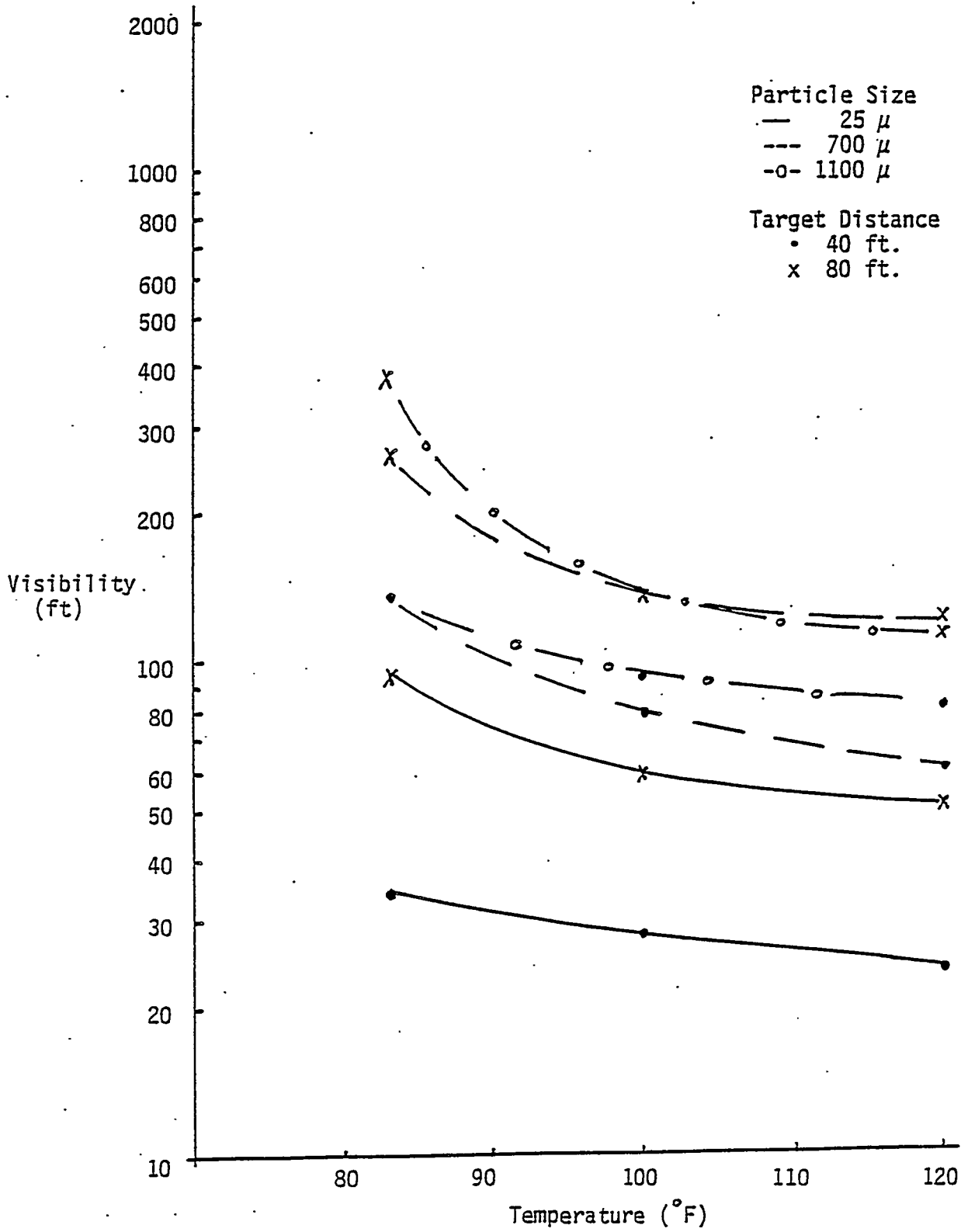


FIGURE 8: Effect of Target Temperature on Visibility Through the Fog with 2- to 5-Micron Infrared Detector

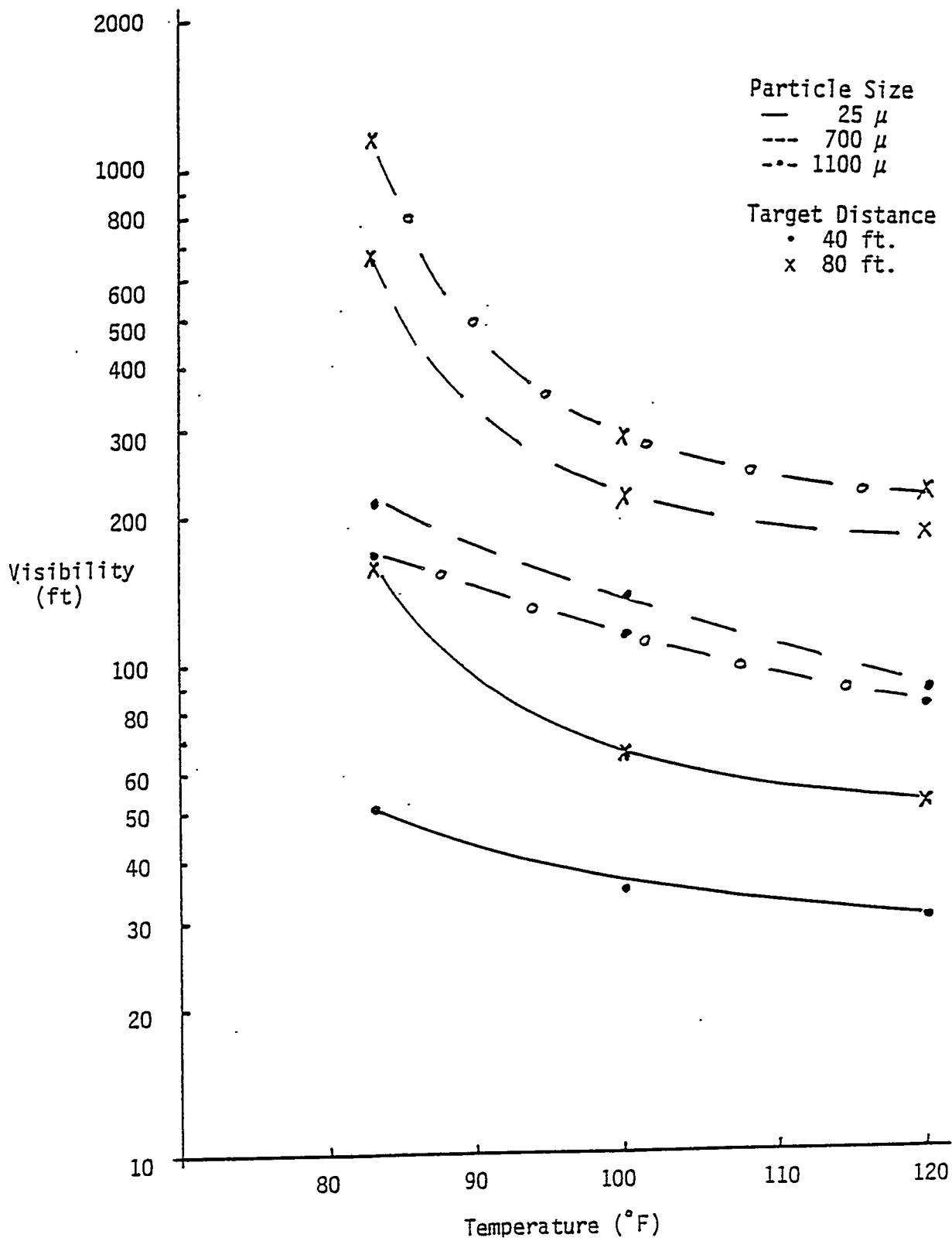


FIGURE 9: Effect of Target Temperature on Visibility Through the Fog with 3- to 5-Micron Infrared Detector

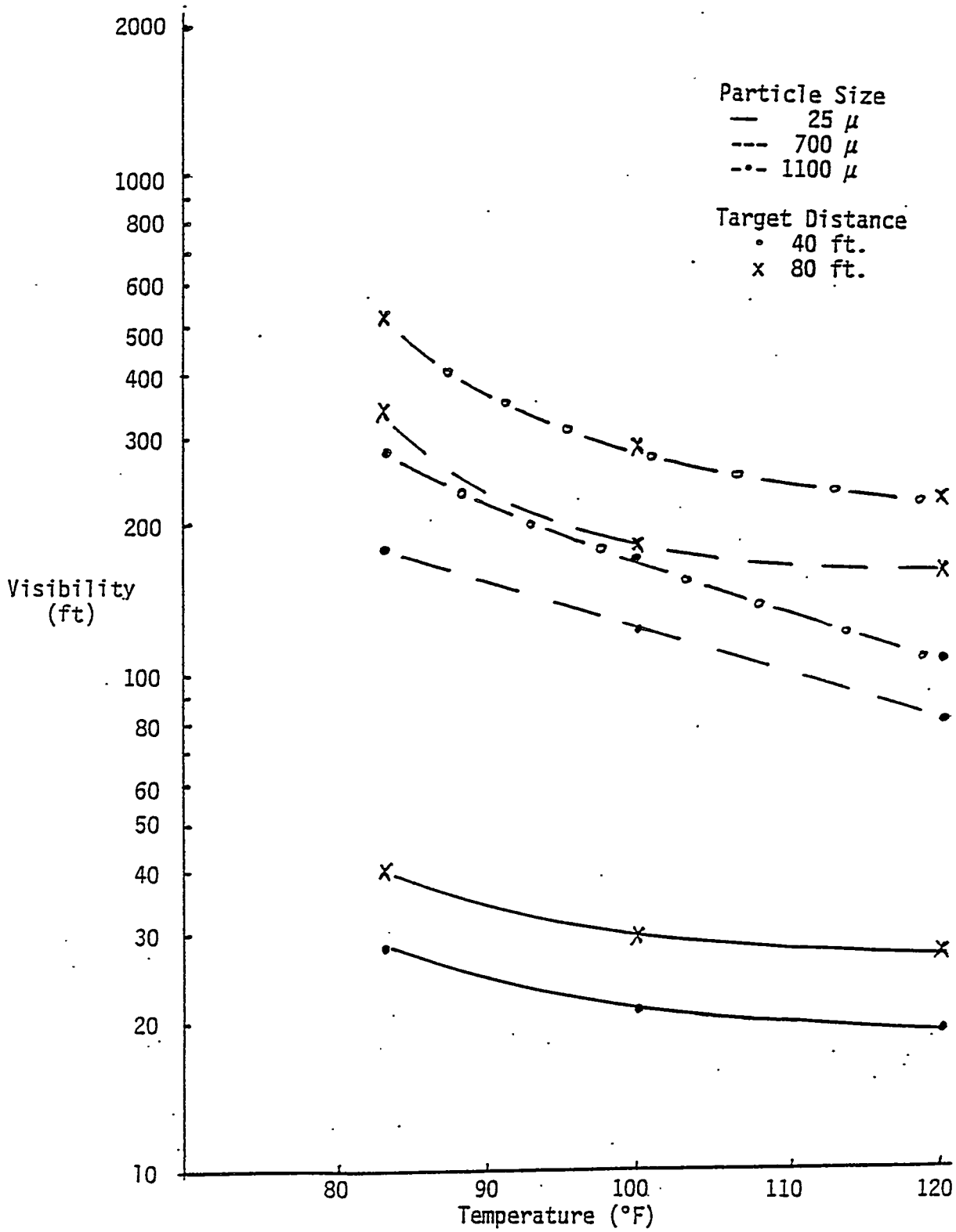


FIGURE 10: Effect of Target Temperature on Visibility Through the Fog with 8- to 12-Micron Infrared Detector

Image enhancement techniques can improve the ability of visible cameras to image through the fog/water droplets. The test results are shown in Tables 9 and 10. The contrast enhancement that was used for this test was used in real-time imaging of the target. Images taken with a CCD camera through a fog or mist generally lack contrast as can be seen in the left images of Figures 11 and 12. The human eye can only resolve about 30 shades of gray; therefore, although there may be a great deal of information about a scene in an image, it may be "lost" due to the limits of our eyes if all the information lies in similar shades of gray. Because a typical gray-scale CCD camera will output 256 different shades of gray, scenes which are low in contrast may only use one small region of the available gray scale. It is possible, therefore, to take a low contrast image and manipulate the gray scale so that the gray levels of the image are expanded and now lay across the entire 256 shade range. This enables us to observe small changes between adjacent shades which would otherwise be invisible. Thus, there is no new information gained by this procedure; however, it does enable a person looking at a video screen to see more detail through fog/water droplets, effectively enhancing their vision.

As a video image is digitized, it is passed through an Input Look Up Table (ILUT) to transform the incoming signal's 256 discrete values to be displayed on the screen. Usually the ILUT is 256 linear increasing values (0=0, 1=1, 2=2, etc.) for normal video, or decreasing values (1=255, 2=254, 3=253, etc.) for inverse video. The ILUT can be manipulated so that only a certain range of values are passed and mapped to spread out values, e.g., 125=0, 126=11, 127=23, etc., which increases their contrast. Results of this treatment for experimental data are encouraging and are shown in Figures 11 and 12. Figure 11 is for a target at 40 feet that is backlighted with the 500-watt tungsten lamp. Figure 12 is for the target at 80 feet that is frontlighted with the same lamp.

Contrast enhancement can be done and the resulting images displayed in real-time. It is very flexible and can be made self-monitoring. One frame can be used to analyze the actual brightness and contrast of the scene, then

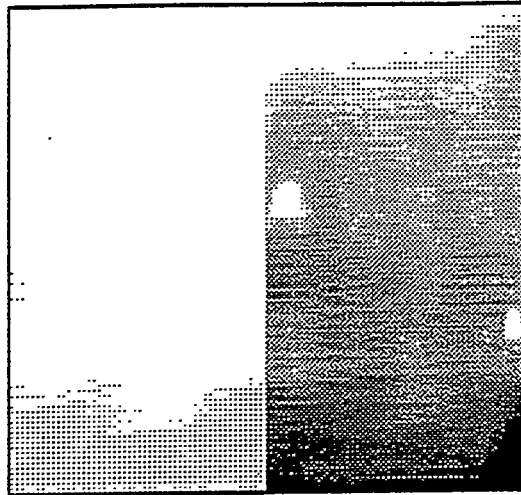
**TABLE 9. Effect of Contrast Enhancement with Target at 40 Feet**

| Detector                | Attenuation*<br>(/ft) |        |        | Visibility*<br>(ft) |     |      | Figure of Merit |       |       |
|-------------------------|-----------------------|--------|--------|---------------------|-----|------|-----------------|-------|-------|
|                         | 25                    | 700    | 1100   | 25                  | 700 | 1100 | 25              | 700   | 1100  |
| Particle Size (Microns) |                       |        |        |                     |     |      |                 |       |       |
| CCD Camera              |                       |        |        |                     |     |      |                 |       |       |
| Visible                 |                       |        |        |                     |     |      |                 |       |       |
| Backlight               | 0.050                 | 0.099  | 0.065  | 60                  | 68  | 103  | 0.67            | 0.59  | 0.39  |
| Frontlight              |                       |        |        |                     |     |      |                 |       |       |
| Room Lights             | 0.076                 | >0.113 | >0.084 | 40                  | <60 | <80  | 1.00            | >0.67 | >0.50 |
| 500 w Bulb              | 0.061                 | >0.113 | >0.084 | 30                  | <60 | <80  | 1.33            | >0.67 | >0.50 |
| Contrast Enhanced       |                       |        |        |                     |     |      |                 |       |       |
| Visible                 |                       |        |        |                     |     |      |                 |       |       |
| Backlight               | 0.061                 | >0.113 | >0.084 | 49                  | <60 | <80  | 0.82            | >0.67 | >0.50 |
| Frontlight              |                       |        |        |                     |     |      |                 |       |       |
| Room Lights             | 0.097                 | >0.113 | >0.084 | 31                  | <60 | <80  | 1.29            | >0.67 | >0.50 |
| 500 w Bulb              | 0.145                 | >0.113 | >0.084 | 27                  | <60 | <80  | 1.48            | >0.67 | >0.50 |

**TABLE 10. Effect of Contrast Enhancement with Target at 80 Feet**

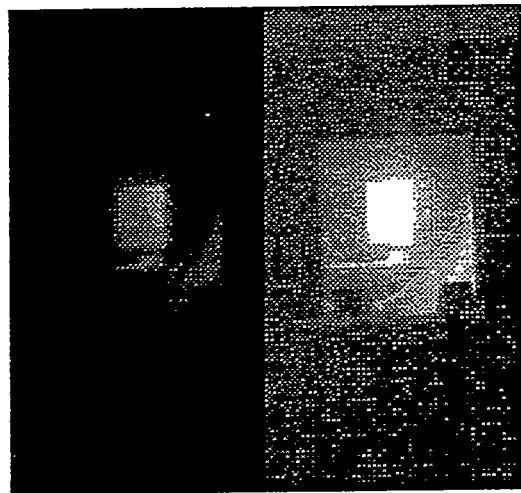
| Detector                | Attenuation*<br>(/ft) |       |       | Visibility*<br>(ft) |     |      | Figure of Merit |      |      |
|-------------------------|-----------------------|-------|-------|---------------------|-----|------|-----------------|------|------|
|                         | 25                    | 700   | 1100  | 25                  | 700 | 1100 | 25              | 700  | 1100 |
| Particle Size (Microns) |                       |       |       |                     |     |      |                 |      |      |
| CCD Camera              |                       |       |       |                     |     |      |                 |      |      |
| Visible                 |                       |       |       |                     |     |      |                 |      |      |
| Frontlight              |                       |       |       |                     |     |      |                 |      |      |
| Room Lights             | 0.038                 | 0.046 | 0.041 | 79                  | 146 | 164  | 1.01            | 0.55 | 0.49 |
| 500 w Bulb              | 0.054                 | 0.078 | 0.073 | 56                  | 86  | 92   | 1.43            | 0.93 | 0.87 |
| Contrast Enhanced       |                       |       |       |                     |     |      |                 |      |      |
| Visible                 |                       |       |       |                     |     |      |                 |      |      |
| Frontlight              |                       |       |       |                     |     |      |                 |      |      |
| Room Lights             | 0.049                 | 0.078 | 0.065 | 62                  | 86  | 103  | 1.29            | 0.93 | 0.78 |
| 500 w Bulb              | 0.059                 | 0.099 | 0.084 | 51                  | 68  | 80   | 1.57            | 1.18 | 1.00 |

\* Attenuation and Visibility measured at 0.63 microns



Target Backlighting.  
Original Image on Left.  
Contrast Enhanced Image on  
Right.

FIGURE 11. Effect of Contrast Enhancement on Visual Image at 40 Feet



Target Frontlighting.  
Original Image on Left.  
Contrast Enhanced Image on  
Right.

FIGURE 12. Effect of Contrast Enhancement on Visual Image at 80 Feet

the contrast can be adjusted to account for changing factors with no more than a "blip" in the real-time display. This can be done automatically at preset time intervals or on demand as the viewer sees fit.

There was no gain in using contrast enhancement for the image produced by the infrared imagers. Only 20 grey scales were available with the infrared imager. With the 20°F temperature gradient used for these tests, there was no improvement noted by using contrast enhancement for the size of target that was tested, which matched the requirements needed for waste tank applications.

Tests were conducted in which salt was added to the water. The results, shown in Tables 11 and 12, indicate that adding salt to the fog/water droplets did not change the visual range through which an object can be viewed. As will be discussed in the section on reproducibility of results, the transmission of the laser beam when the object first became visible fell within the measurement error when comparing the results with and without salt added to the fog/water droplets. This test was performed by adding 20% salt by weight to tap water. It was observed that the fog would not dissipate as quickly with the salt in it as it did with no salt in it.

#### Reproducibility of Results

In the course of these tests, several tests were repeated at various times. From the results of these approximately 12 tests, it was determined that the average error in measuring the transmission of the fog when the target was just identifiable was +1.7%. This would lead to an error of +4 feet in measuring the visibility through the fog, and  $\pm 12$  ft in measuring the visibility through the water droplets (at a target distance of 40 feet).

#### 3.2.2. Acoustic Sensors

Acoustic sensors are generally divided into two categories: electrostatic transducers and piezoelectric transducers. A sample of each of these transducers was used for the tests in this project.

**TABLE 11. Comparison of the Effect of Adding Salt to Fog/Water Droplets at 40 Feet Target Distance**

| Wavelength Region       | No Salt Added to the Water |                  |                 | 20% Salt Added to the Water |                  |                 |
|-------------------------|----------------------------|------------------|-----------------|-----------------------------|------------------|-----------------|
|                         | Attenuation* (/ft)         | Visibility* (ft) | Figure of Merit | Attenuation* (/ft)          | Visibility* (ft) | Figure of Merit |
| Particle Size (microns) | 25                         | 700              | 1100            | 25                          | 700              | 1100            |
| Visible Backlight       | 0.050                      | 0.099            | 0.065           | 60                          | 68               | 103             |
| Frontlight              | >0.113                     | >0.084           | 40              | <60                         | <80              | 3.0             |
| Room Lights             | >0.113                     | >0.084           | 30              | <60                         | <80              | 0.9             |
| 500 w Bulb              | 0.107                      | 0.038            | 0.024           | 28                          | 177              | 280             |
| 8-12 Micron             |                            |                  |                 | 0.045                       | 0.089            | 0.065           |
|                         |                            |                  |                 | 0.039                       | 0.059            | 0.067           |
|                         |                            |                  |                 | 0.088                       | >0.070           | 34              |
|                         |                            |                  |                 | 0.118                       | >0.070           | 26              |
|                         |                            |                  |                 | 0.030                       | 0.027            | 34              |
|                         |                            |                  |                 | 0.027                       | 34               | 224             |
|                         |                            |                  |                 | 0.065                       | 67               | 103             |
|                         |                            |                  |                 | 0.089                       | >0.070           | 34              |
|                         |                            |                  |                 | 0.095                       | >0.070           | 26              |
|                         |                            |                  |                 | 0.030                       | 0.027            | 34              |
|                         |                            |                  |                 | 0.027                       | 34               | 224             |
|                         |                            |                  |                 | 0.065                       | 67               | 103             |
|                         |                            |                  |                 | 0.089                       | >0.070           | 34              |
|                         |                            |                  |                 | 0.095                       | >0.070           | 26              |
|                         |                            |                  |                 | 0.030                       | 0.027            | 34              |
|                         |                            |                  |                 | 0.027                       | 34               | 224             |
|                         |                            |                  |                 | 0.065                       | 67               | 103             |
|                         |                            |                  |                 | 0.089                       | >0.070           | 34              |
|                         |                            |                  |                 | 0.095                       | >0.070           | 26              |
|                         |                            |                  |                 | 0.030                       | 0.027            | 34              |
|                         |                            |                  |                 | 0.027                       | 34               | 224             |
|                         |                            |                  |                 | 0.065                       | 67               | 103             |
|                         |                            |                  |                 | 0.089                       | >0.070           | 34              |
|                         |                            |                  |                 | 0.095                       | >0.070           | 26              |
|                         |                            |                  |                 | 0.030                       | 0.027            | 34              |
|                         |                            |                  |                 | 0.027                       | 34               | 224             |
|                         |                            |                  |                 | 0.065                       | 67               | 103             |
|                         |                            |                  |                 | 0.089                       | >0.070           | 34              |
|                         |                            |                  |                 | 0.095                       | >0.070           | 26              |
|                         |                            |                  |                 | 0.030                       | 0.027            | 34              |
|                         |                            |                  |                 | 0.027                       | 34               | 224             |
|                         |                            |                  |                 | 0.065                       | 67               | 103             |
|                         |                            |                  |                 | 0.089                       | >0.070           | 34              |
|                         |                            |                  |                 | 0.095                       | >0.070           | 26              |
|                         |                            |                  |                 | 0.030                       | 0.027            | 34              |
|                         |                            |                  |                 | 0.027                       | 34               | 224             |
|                         |                            |                  |                 | 0.065                       | 67               | 103             |
|                         |                            |                  |                 | 0.089                       | >0.070           | 34              |
|                         |                            |                  |                 | 0.095                       | >0.070           | 26              |
|                         |                            |                  |                 | 0.030                       | 0.027            | 34              |
|                         |                            |                  |                 | 0.027                       | 34               | 224             |
|                         |                            |                  |                 | 0.065                       | 67               | 103             |
|                         |                            |                  |                 | 0.089                       | >0.070           | 34              |
|                         |                            |                  |                 | 0.095                       | >0.070           | 26              |
|                         |                            |                  |                 | 0.030                       | 0.027            | 34              |
|                         |                            |                  |                 | 0.027                       | 34               | 224             |
|                         |                            |                  |                 | 0.065                       | 67               | 103             |
|                         |                            |                  |                 | 0.089                       | >0.070           | 34              |
|                         |                            |                  |                 | 0.095                       | >0.070           | 26              |
|                         |                            |                  |                 | 0.030                       | 0.027            | 34              |
|                         |                            |                  |                 | 0.027                       | 34               | 224             |
|                         |                            |                  |                 | 0.065                       | 67               | 103             |
|                         |                            |                  |                 | 0.089                       | >0.070           | 34              |
|                         |                            |                  |                 | 0.095                       | >0.070           | 26              |
|                         |                            |                  |                 | 0.030                       | 0.027            | 34              |
|                         |                            |                  |                 | 0.027                       | 34               | 224             |
|                         |                            |                  |                 | 0.065                       | 67               | 103             |
|                         |                            |                  |                 | 0.089                       | >0.070           | 34              |
|                         |                            |                  |                 | 0.095                       | >0.070           | 26              |
|                         |                            |                  |                 | 0.030                       | 0.027            | 34              |
|                         |                            |                  |                 | 0.027                       | 34               | 224             |
|                         |                            |                  |                 | 0.065                       | 67               | 103             |
|                         |                            |                  |                 | 0.089                       | >0.070           | 34              |
|                         |                            |                  |                 | 0.095                       | >0.070           | 26              |
|                         |                            |                  |                 | 0.030                       | 0.027            | 34              |
|                         |                            |                  |                 | 0.027                       | 34               | 224             |
|                         |                            |                  |                 | 0.065                       | 67               | 103             |
|                         |                            |                  |                 | 0.089                       | >0.070           | 34              |
|                         |                            |                  |                 | 0.095                       | >0.070           | 26              |
|                         |                            |                  |                 | 0.030                       | 0.027            | 34              |
|                         |                            |                  |                 | 0.027                       | 34               | 224             |
|                         |                            |                  |                 | 0.065                       | 67               | 103             |
|                         |                            |                  |                 | 0.089                       | >0.070           | 34              |
|                         |                            |                  |                 | 0.095                       | >0.070           | 26              |
|                         |                            |                  |                 | 0.030                       | 0.027            | 34              |
|                         |                            |                  |                 | 0.027                       | 34               | 224             |
|                         |                            |                  |                 | 0.065                       | 67               | 103             |
|                         |                            |                  |                 | 0.089                       | >0.070           | 34              |
|                         |                            |                  |                 | 0.095                       | >0.070           | 26              |
|                         |                            |                  |                 | 0.030                       | 0.027            | 34              |
|                         |                            |                  |                 | 0.027                       | 34               | 224             |
|                         |                            |                  |                 | 0.065                       | 67               | 103             |
|                         |                            |                  |                 | 0.089                       | >0.070           | 34              |
|                         |                            |                  |                 | 0.095                       | >0.070           | 26              |
|                         |                            |                  |                 | 0.030                       | 0.027            | 34              |
|                         |                            |                  |                 | 0.027                       | 34               | 224             |
|                         |                            |                  |                 | 0.065                       | 67               | 103             |
|                         |                            |                  |                 | 0.089                       | >0.070           | 34              |
|                         |                            |                  |                 | 0.095                       | >0.070           | 26              |
|                         |                            |                  |                 | 0.030                       | 0.027            | 34              |
|                         |                            |                  |                 | 0.027                       | 34               | 224             |
|                         |                            |                  |                 | 0.065                       | 67               | 103             |
|                         |                            |                  |                 | 0.089                       | >0.070           | 34              |
|                         |                            |                  |                 | 0.095                       | >0.070           | 26              |
|                         |                            |                  |                 | 0.030                       | 0.027            | 34              |
|                         |                            |                  |                 | 0.027                       | 34               | 224             |
|                         |                            |                  |                 | 0.065                       | 67               | 103             |
|                         |                            |                  |                 | 0.089                       | >0.070           | 34              |
|                         |                            |                  |                 | 0.095                       | >0.070           | 26              |
|                         |                            |                  |                 | 0.030                       | 0.027            | 34              |
|                         |                            |                  |                 | 0.027                       | 34               | 224             |
|                         |                            |                  |                 | 0.065                       | 67               | 103             |
|                         |                            |                  |                 | 0.089                       | >0.070           | 34              |
|                         |                            |                  |                 | 0.095                       | >0.070           | 26              |
|                         |                            |                  |                 | 0.030                       | 0.027            | 34              |
|                         |                            |                  |                 | 0.027                       | 34               | 224             |
|                         |                            |                  |                 | 0.065                       | 67               | 103             |
|                         |                            |                  |                 | 0.089                       | >0.070           | 34              |
|                         |                            |                  |                 | 0.095                       | >0.070           | 26              |
|                         |                            |                  |                 | 0.030                       | 0.027            | 34              |
|                         |                            |                  |                 | 0.027                       | 34               | 224             |
|                         |                            |                  |                 | 0.065                       | 67               | 103             |
|                         |                            |                  |                 | 0.089                       | >0.070           | 34              |
|                         |                            |                  |                 | 0.095                       | >0.070           | 26              |
|                         |                            |                  |                 | 0.030                       | 0.027            | 34              |
|                         |                            |                  |                 | 0.027                       | 34               | 224             |
|                         |                            |                  |                 | 0.065                       | 67               | 103             |
|                         |                            |                  |                 | 0.089                       | >0.070           | 34              |
|                         |                            |                  |                 | 0.095                       | >0.070           | 26              |
|                         |                            |                  |                 | 0.030                       | 0.027            | 34              |
|                         |                            |                  |                 | 0.027                       | 34               | 224             |
|                         |                            |                  |                 | 0.065                       | 67               | 103             |
|                         |                            |                  |                 | 0.089                       | >0.070           | 34              |
|                         |                            |                  |                 | 0.095                       | >0.070           | 26              |
|                         |                            |                  |                 | 0.030                       | 0.027            | 34              |
|                         |                            |                  |                 | 0.027                       | 34               | 224             |
|                         |                            |                  |                 | 0.065                       | 67               | 103             |
|                         |                            |                  |                 | 0.089                       | >0.070           | 34              |
|                         |                            |                  |                 | 0.095                       | >0.070           | 26              |
|                         |                            |                  |                 | 0.030                       | 0.027            | 34              |
|                         |                            |                  |                 | 0.027                       | 34               | 224             |
|                         |                            |                  |                 | 0.065                       | 67               | 103             |
|                         |                            |                  |                 | 0.089                       | >0.070           | 34              |
|                         |                            |                  |                 | 0.095                       | >0.070           | 26              |
|                         |                            |                  |                 | 0.030                       | 0.027            | 34              |
|                         |                            |                  |                 | 0.027                       | 34               | 224             |
|                         |                            |                  |                 | 0.065                       | 67               | 103             |
|                         |                            |                  |                 | 0.089                       | >0.070           | 34              |
|                         |                            |                  |                 | 0.095                       | >0.070           | 26              |
|                         |                            |                  |                 | 0.030                       | 0.027            | 34              |
|                         |                            |                  |                 | 0.027                       | 34               | 224             |
|                         |                            |                  |                 | 0.065                       | 67               | 103             |
|                         |                            |                  |                 | 0.089                       | >0.070           | 34              |
|                         |                            |                  |                 | 0.095                       | >0.070           | 26              |
|                         |                            |                  |                 | 0.030                       | 0.027            | 34              |
|                         |                            |                  |                 | 0.027                       | 34               | 224             |
|                         |                            |                  |                 | 0.065                       | 67               | 103             |
|                         |                            |                  |                 | 0.089                       | >0.070           | 34              |
|                         |                            |                  |                 | 0.095                       | >0.070           | 26              |
|                         |                            |                  |                 | 0.030                       | 0.027            | 34              |
|                         |                            |                  |                 | 0.027                       | 34               | 224             |
|                         |                            |                  |                 | 0.065                       | 67               | 103             |
|                         |                            |                  |                 | 0.089                       | >0.070           | 34              |
|                         |                            |                  |                 | 0.095                       | >0.070           | 26              |
|                         |                            |                  |                 | 0.030                       | 0.027            | 34              |
|                         |                            |                  |                 | 0.027                       | 34               | 224             |
|                         |                            |                  |                 | 0.065                       | 67               | 103             |
|                         |                            |                  |                 | 0.089                       | >0.070           | 34              |
|                         |                            |                  |                 | 0.095                       | >0.070           | 26              |
|                         |                            |                  |                 | 0.030                       | 0.027            | 34              |
|                         |                            |                  |                 | 0.027                       | 34               | 224             |
|                         |                            |                  |                 | 0.065                       | 67               | 103             |
|                         |                            |                  |                 | 0.089                       | >0.070           | 34              |
|                         |                            |                  |                 | 0.095                       | >0.070           | 26              |
|                         |                            |                  |                 | 0.030                       | 0.027            | 34              |
|                         |                            |                  |                 | 0.027                       | 34               | 224             |
|                         |                            |                  |                 | 0.065                       | 67               | 103             |
|                         |                            |                  |                 | 0.089                       | >0.070           | 34              |
|                         |                            |                  |                 | 0.095                       | >0.070           | 26              |
|                         |                            |                  |                 | 0.030                       | 0.027            | 34              |
|                         |                            |                  |                 | 0.027                       | 34               | 224             |
|                         |                            |                  |                 | 0.065                       | 67               | 103             |
|                         |                            |                  |                 | 0.089                       | >0.070           | 34              |
|                         |                            |                  |                 | 0.095                       | >0.070           | 26              |
|                         |                            |                  |                 | 0.030                       | 0.027            | 34              |
|                         |                            |                  |                 | 0.027                       | 34               | 224             |
|                         |                            |                  |                 | 0.065                       | 67               | 103             |
|                         |                            |                  |                 | 0.089                       | >0.070           | 34              |
|                         |                            |                  |                 | 0.095                       | >0.070           | 26              |
|                         |                            |                  |                 | 0.030                       | 0.027            | 34              |
|                         |                            |                  |                 | 0.027                       | 34               | 224             |
|                         |                            |                  |                 | 0.065                       | 67               | 103             |
|                         |                            |                  |                 | 0.089                       | >0.070           | 34              |
|                         |                            |                  |                 | 0.095                       | >0.070           | 26              |
|                         |                            |                  |                 | 0.030                       | 0.027            | 34              |
|                         |                            |                  |                 | 0.027                       | 34               | 224             |
|                         |                            |                  |                 | 0.065                       | 67               | 103             |
|                         |                            |                  |                 | 0.089                       | >0.070           | 34              |
|                         |                            |                  |                 | 0.095                       | >0.070           | 26              |
|                         |                            |                  |                 | 0.030                       | 0.027            | 34              |
|                         |                            |                  |                 | 0.027                       | 34               | 224             |
|                         |                            |                  |                 | 0.065                       | 67               | 103             |
|                         |                            |                  |                 | 0.089                       | >0.070           | 34              |
|                         |                            |                  |                 | 0.095                       | >0.070           | 26              |
|                         |                            |                  |                 | 0.030                       | 0.027            | 34              |
|                         |                            |                  |                 | 0.027                       | 34               | 224             |
|                         |                            |                  |                 | 0.065                       | 67               | 103             |
|                         |                            |                  |                 | 0.089                       | >0.070           | 34              |
|                         |                            |                  |                 | 0.095                       | >0.070           | 26              |
|                         |                            |                  |                 | 0.030                       | 0.027            | 34              |
|                         |                            |                  |                 | 0.027                       | 34               | 224             |
|                         |                            |                  |                 | 0.065                       | 67               | 103             |
|                         |                            |                  |                 | 0.089                       | >0.070           | 34              |
|                         |                            |                  |                 | 0.095                       | >0.070           | 26              |
|                         |                            |                  |                 | 0.030                       | 0.027            | 34              |
|                         |                            |                  |                 | 0.027                       | 34               | 224             |
|                         |                            |                  |                 |                             |                  |                 |

Electrostatic transducers operate by using an electrostatic force to move a thin, usually plastic (Kapton) foil. An AC voltage of a given frequency causes the foil to move at the same frequency and to transmit an energy wave. Piezoelectric transducers operate on the same principle; however, instead of a moving foil, a piezoelectric crystal is excited.

Generally, the electrostatic transducers will work for longer distances. The problem with them is that they do not function well in harsh environments because moisture will condense on the open foil, causing it to fail. In addition, they are usually not sealed as well as the piezoelectric sensors. Some manufacturers eliminate this problem by blowing air through the transducer and concentrating horn, if they have one; some of the devices have fittings for attaching air lines. The electrostatic transducer was used for this test series because it operated for a longer distance than the piezoelectric transducers.

The electrostatic transducer that was used for these tests was the acoustic sensor used in the Polaroid camera. It had a range of 35 feet and operates with a chirp frequency around 50 kHz. The piezoelectric transducer that was used in these tests was manufactured by Lundahl Instruments, Inc., (Model DCU-7) and also operated at approximately 50 kHz. It was chosen because it was designed to operate in harsh environments, and with a horn attached to it, had a narrow beam divergence ( $\pm 1.7^\circ$ ). Its range was only 10 feet. In addition, a piezoelectric transducer manufactured by Micro Switch, Inc., (Model 942) was also tested. It operated at 215 kHz and had a range of about five feet.

### Test Results

The results of the tests indicated that the acoustic sensors that operated at 50 kHz could not operate in the waste tank during sluicing operation because of the acoustic noise. Using a flat metal target set at approximately 9 feet, the Lundahl acoustic sensor exhibited an error of 20 inches when either the air from the fog nozzles was started or the water spray from the 300-micron nozzles was turned on. In addition, the range value was unsteady, varying randomly about  $\pm 1.62$  inches. The same effect was noticed with the Polaroid acoustic sensor. However, with this sensor, it was

possible to set the sensitivity low enough so that it would detect the distance to the metal target. The problem with this is that the sensor would then need a high reflector, e.g., a flat metal target, in order to determine the distance to the target. Observing the signal on an oscilloscope indicates that random white noise was being received by the sensor due to air flow through the nozzles. The sluicing operation can be expected to be noisy, with a high-power water jet operating inside a steel waste tank that contains other apparatus, such as ventilation fans. Therefore, it appears that an acoustic sensor operating near 50 kHz could not be used for waste tank imaging.

The effect of acoustic noise on the ability of the acoustic sensor to detect distance to a target was not observed with the Micro Switch acoustic sensor, which operated at 215 kHz. The distance to a flat metal target approximately five feet away from the sensor increased 0.5 inch when the air turbulence, fog, or 700-micron diameter water spray was started, and the distance varied  $\pm 0.15$  inch. Because the range of this sensor was only about five feet, the test set-up was modified in order to determine the effect of fog and water spray on this transducer. One sensor was placed on one end of the test chamber and was used to transmit the sonic beam; the other sensor was placed in the test chamber to receive the sonic beam. The results of these tests indicate that the acoustic sensor operating at 215 kHz is able to penetrate the fog/water droplets if it has enough power. However, the acoustic wave is attenuated by the fog and water droplets; it was possible for the fog or water droplets to completely attenuate the acoustic beam when these sensors were 10-12 feet apart. Previous tests with this Micro Switch sensor indicated that the sensor lost about 0.071 db/foot as the humidity in a controlled environmental chamber increased from 25% to 95% while the temperature was held at 100°F (Peters et al. 1991). With a target at 80 feet, the pulse-echo signal would travel 160 feet, and the signal would be decreased by 11.4 db, or approximately 75%. When the sensors were seven feet apart, it was possible to get the beam through the fog/water droplets without changing the voltage measured by the sensor. Adding salt to the water did not change the results with the acoustic sensor. Thus, a more powerful acoustic sensor than available commercially, which operated at a few hundred kHz, would be needed for use in the waste tanks. An array of sensors, or scanning one

acoustic sensor, would be needed in order to obtain the required accuracy. For example, if one wants to resolve three inches at 75 feet, the acoustic sensor operating at 215 kHz would need to be approximately 23 inches in diameter.

### 3.2.3 Wideband Millimeter Wave Imaging Technique

A wideband millimeter-wave imaging technique has been developed by PNL for the detection of concealed weapons carried by personnel through high-security areas, such as airports for the United States Federal Aviation Administration (FAA). This technique, similar to an extremely high-resolution radar system, actively probes the target with millimeter waves and reconstructs an image from the backscattered phase and amplitude data. The method used is similar to synthetic aperture radar (SAR) methods in configuration, but differs in that wide bandwidths are swept and targets are imaged near to the scanned aperture. Since the data is collected in the frequency domain and in an unfocused manner, computer reconstruction is required to form a focused image. This imaging technique follows the reconstruction methods given by Soumekh (1991). The reconstruction method begins by taking the recorded amplitude and phase data and performing a Fourier Transform in the lateral direction, which decomposes the wave front into plane wave components. An interpolation is used to obtain uniform samples of the targets reflectivity in the spatial frequency domain. A two-dimensional inverse Fourier Transform is then used to reconstruct the image. This reconstruction algorithm has been simplified for use in this specific application, and the theory of the technique is discussed in Appendix D.

The differences between the wideband millimeter wave imaging technique used in this study and Synthetic Aperture Radar (SAR) is that the wideband millimeter wave imaging technique violates assumptions made in conventional SAR focusing algorithms. However, as in a conventional SAR system, the bandwidth provides range resolution and the lateral aperture provides cross-range resolution. An experimental system has been developed at PNL which has gathered millimeter wave imaging data. This imaging system allows for the formation of a two-dimensional image from a one-dimensional, linearly scanned bistatic transceiver.

Radar imaging techniques form an image using reflected electromagnetic waves. Most conventional radars form an image by mechanically sweeping a relatively narrow beam-width, time-gated beam. Much higher resolution can be obtained using SAR techniques in which a relatively wide, beam-width antenna is scanned over a large linear aperture and focusing is performed in post-processing.

### Test Results

Attenuation Measurements. The measurements were conducted using a W-band (75-110 GHz) transceiver that was configured to operate at a center frequency of 94 GHz and a bandwidth of 1 GHz. This would result in a range resolution of approximately 15 cm. Separate transmit and receive horns were used, each with a gain of 25 dBi and beam-width of approximately  $10^\circ$ . The transceiver operates in a linear swept-frequency mode or a frequency-modulated continuous wave mode. In this mode, the frequency of the IF signal is proportional to the range to the target; therefore, the Fourier Transform of the IF signal will give the range profile of the target(s). Figure 13 shows the imaging front end used in the obscurant attenuation measurements and the preliminary linear aperture imaging studies. This system can be fabricated into a miniaturized package for insertion into the waste tank.

The results of the attenuation measurements are summarized in Table 13. For these tests, a trihedral (corner cube) target was set up 40 feet from the millimeter wave antenna. A pulse was emitted from one antenna, reflected from the trihedral target, and then received by the other antenna. These results indicate that scattering, or attenuation, of the millimeter waves increases as the water particle size increases. The attenuation of the millimeter waves in salt water (20% salt added to water by weight) are nearly identical to the pure water results, indicating that salt or other electrolytes in the water are unlikely to be a factor for millimeter wave imaging. Further testing indicated that millimeter waves are not affected by salt in the water above 8 GHz, which is shown in Figure 14.

The typical target signal was 30-40 dB above the noise. Figure 15 shows the reflective frequency response from the trihedral target during the pulse echo attenuation measurements for the salty fog.

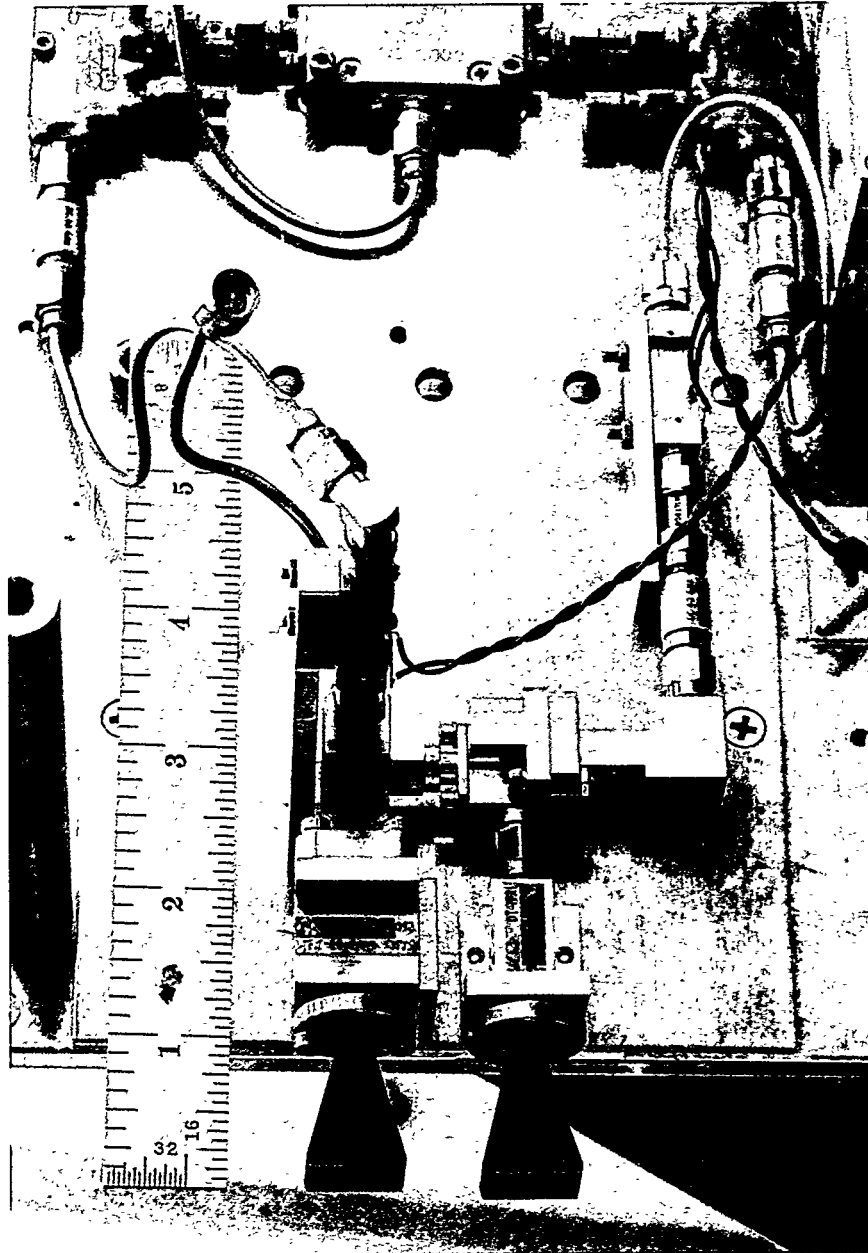


FIGURE 13. Front End Electronics for Millimeter Wave Technique

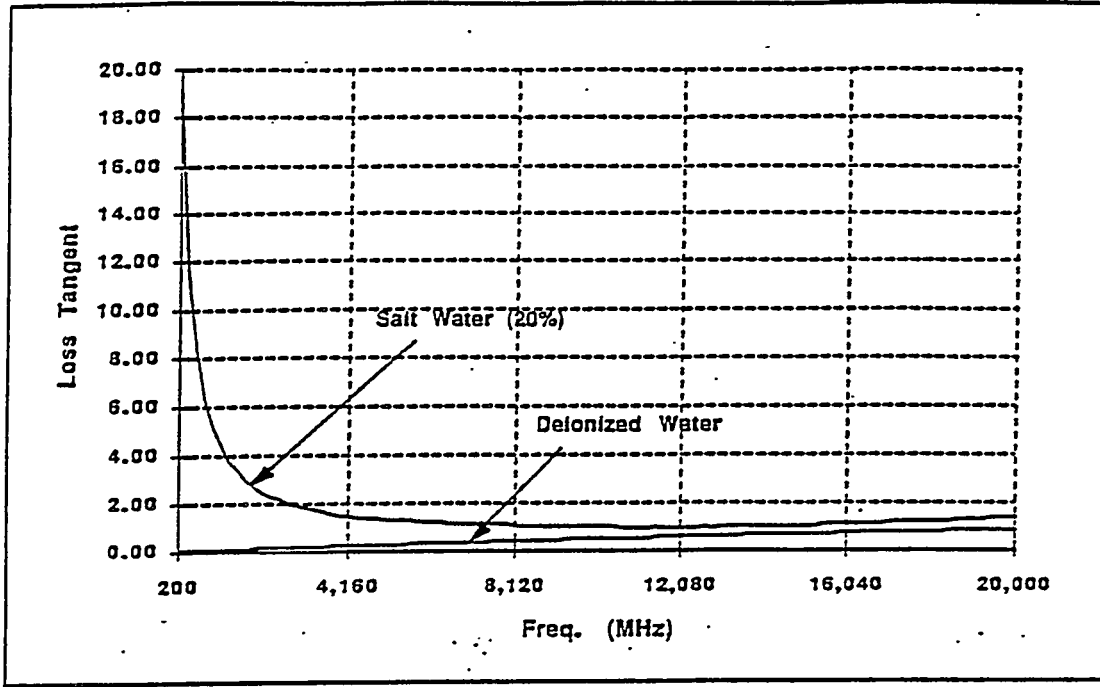


FIGURE 14. Comparison of Loss Tangent of Deionized and Salt Water

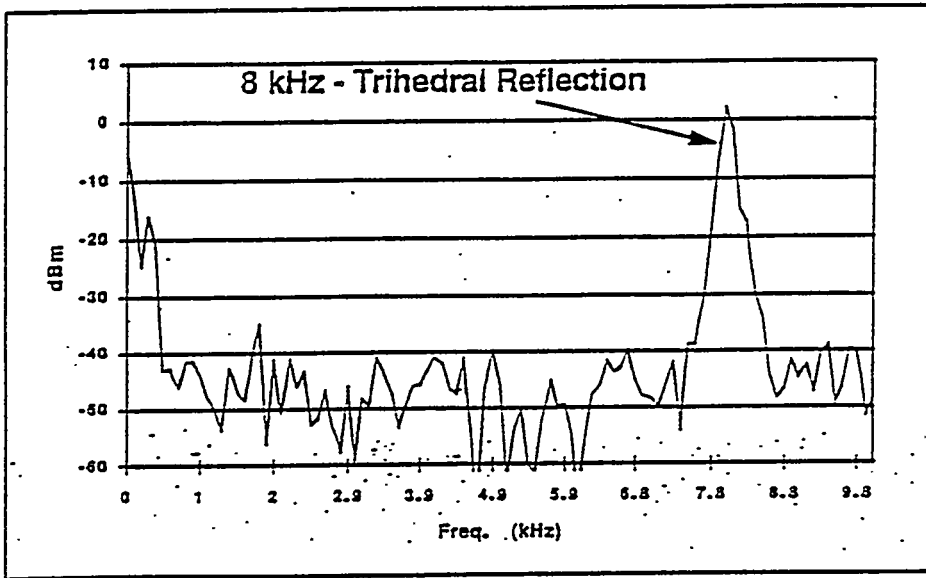


FIGURE 15: Frequency Response from Trihedral Reflector in Test Chamber Filled with 25-Micron Diameter Salt Water

**TABLE 13.** Results of Millimeter Wave Attenuation Measurements at 94 GHz

| Particle Size<br>(Microns) | Attenuation (dBm) |            |                |            | Net Loss |            |       |            |
|----------------------------|-------------------|------------|----------------|------------|----------|------------|-------|------------|
|                            | Chamber Empty     |            | Chamber Filled |            | dB       |            | dB/ft |            |
|                            | Water             | Salt Water | Water          | Salt Water | Water    | Salt Water | Water | Salt Water |
| 25                         | 3.1               | 3.9        | 1.6            | 2.7        | 1.5      | 1.2        | 0.018 | 0.015      |
| 700                        | 3.2               | 4.9        | -3.3           | -2.0       | 6.5      | 6.6        | 0.082 | 0.082      |
| 1100                       | 2.9               | 3.6        | -5.5           | -5.2       | 8.4      | 8.8        | 0.100 | 0.110      |

Imaging Tests. An experimental system, shown in Figure 16, was assembled to gather data for the wideband linearly scanned imaging technique. This system utilizes a 6-foot by 6-foot high-resolution x-y scanner. Typically, only the horizontal direction is used for this imaging configuration. The transceiver for these preliminary imaging studies used a heterodyne receiver configuration operating at a frequency range from 95 to 115 GHz. Separate transmit and receive horn antennas are directed at the target, as shown in Figure 17, and an inclination angle is used to provide adequate illumination of the target. During scans, data from the transceiver is downloaded to a computer for subsequent image reconstruction.

Since resolution cell size in the y-direction is inversely proportional to bandwidth, it is extremely desirable to use the widest possible bandwidth. The transceiver that performed these preliminary images was designed and fabricated for another project with range requirements of six to ten feet. The number of sampling points required for this range and bandwidth is 800 points. The number of sampling points used, however, was 1024 to allow a maximum non-aliased range of 12.6 feet for the 95-115 GHz frequency range.

A single antenna can be used for both transmit and receive with a directional coupler used to separate the signals. However, significantly better performance is achieved by using separate antennas for transmit and receive, and then recording the transmission from the transmit to the receive antenna. If the antennas are small and placed close to each other, the transmission signal is equivalent to the reflected signal from a monostatic arrangement. However, internal cabling impedance mismatches and the antenna

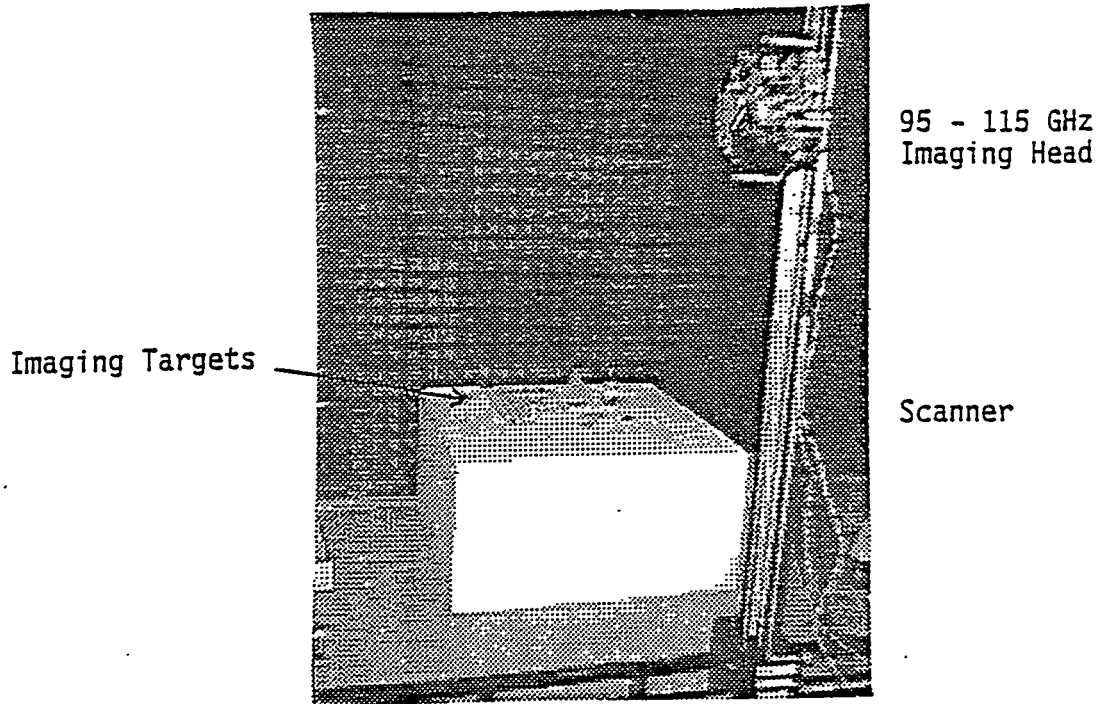


FIGURE 16. Experimental Set-Up of Millimeter Wave Imaging System

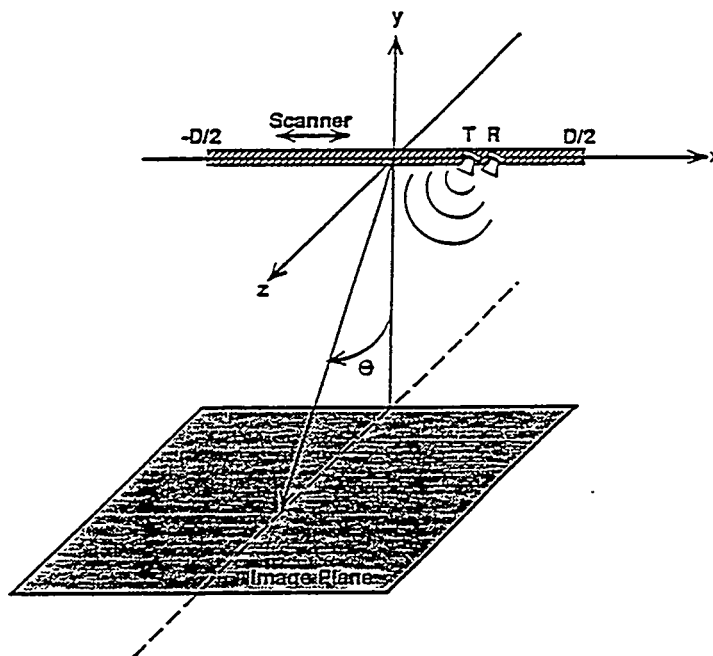


FIGURE 17. Experimental W-Band System Configuration

impedance mismatch will not be present in the detected signal. This is very important as these signals can be quite large relative to the reflected signals in the monostatic arrangement. There will still be an undesirable signal coupled from the transmit to the receive antenna. This signal is not very strong, and may be removed easily by software time-gating the Fourier Transform of the wideband response.

The scanner provides a maximum aperture of approximately four feet. At each  $x$  position (see Figure 17), a full frequency sweep is performed and the measured results are downloaded to the computer. A general purpose SUN 4/370 was used to control the scanner and record the data. After data collection, a SKY i860 coprocessor is used to reconstruct the image. Presently, reconstruction of a 512 x 1024 pixel image takes approximately 20 seconds. This time can be significantly reduced by optimizing the algorithm and size of the data and image.

To adequately illuminate the target over the full  $y$ -direction extent (up to 10 feet), it is necessary to incline the antennas to approximately  $30^\circ$ . This is done to prevent portions of the target from shadowing other portions of the target. This will reduce the  $y$  resolution by a small amount in accordance with equation 17 in Appendix D. The expected resolution for the 95-115 GHz system is  $d_x$ , equal to approximately 0.14 inch ( $F\#=2.5$ ), and  $d_y$ , equal to approximately 0.59 inch, for a horizontal aperture of 4 feet, range of 10 feet, and slant angle of  $30^\circ$ .

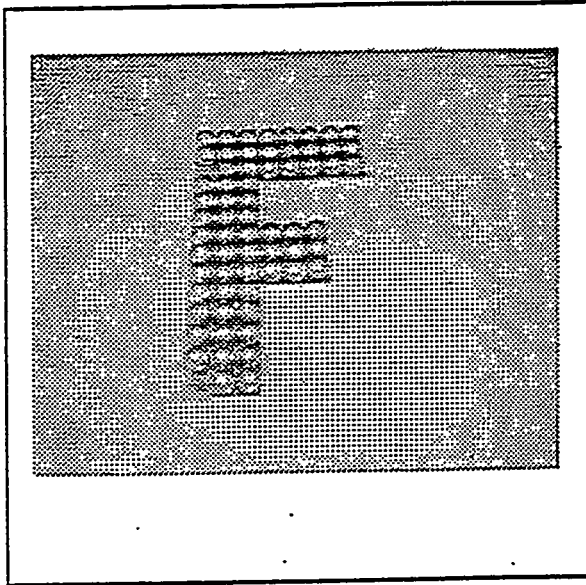
A test target was fabricated to demonstrate the resolution and focusing capabilities of the experimental imaging system and reconstruction algorithm. This test target is in the form of an uppercase block letter "F" which is composed of three rows of metallized spheres. The spheres are 1.5 inches in diameter. Spheres were used in the fabrication of this test target since they have a uniform response in the backscatter direction at all angles. Thus, each sphere in the target should generate a significant return at each scanner position. Data was obtained from this target with a 95-115 GHz frequency range at 512 points uniformly spaced along a 4-foot horizontal aperture. The angle of illumination is approximately  $30^\circ$ . Image processing algorithms were applied to the  $x$ ,  $k_x$ , and  $k_y$  axes to reduce side-lobes. The reconstructed

image is displayed in Figure 18 along with an optical image for comparison. Because of the power output of the millimeter wave antenna (0.2 mw) that was available for these tests, it was not possible to image objects beyond a range of 6 to 10 feet. This result demonstrates high resolution on the order of 1.5 inches, and demonstrates the effectiveness of the transceiver and image-reconstruction algorithm.

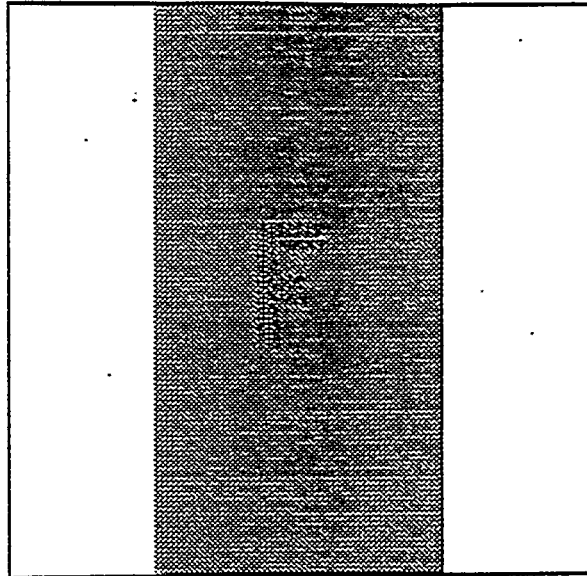
Figure 19 shows other test targets used for preliminary millimeter wave imaging tests. The targets include two test objects in the form of an uppercase block letter "F" where one is composed of three rows of 1.5-inch diameter metallized spheres and the other is composed two rows of 0.75-inch diameter metallized spheres. Other targets include two glass bottles. A glass target was used because glass has a relative permittivity (compared to empty space) of 4-10 (Weast 1976-1977, p. E-60). This is similar to the relative permittivity of sodium nitrate, which is 5.2, and sodium carbonate, which is 5-8 (Weast 1976-1977, p.E-58), which are two major constituents in the waste tanks. Water, another major constituent, has a relative permittivity of approximately 80 at room temperature (Weast 1976-1977, p. E-61). The amount of energy reflected from the target surface is a function of the permittivity and conductivity of the surface. The glass bottle closest to the two "Fs" is filled with water, the other is empty. A bottle cap is to the right of the smaller "F". The optical image is included to compare the results.

Figure 20 shows the imaging results for the small plastic wading pool filled with water. Duct putty mounds are protruding out of the water in the pool's center and are also placed on the pool's outer rim. The optical image is shown for comparison. Comparing Figures 19 and 20 shows that a rough target, like duct putty, produces a millimeter wave image that more closely represents the object than a smooth cylindrical target, such as the glass bottle. It would be expected that the waste tank contents would be a rough target.

Conceptual Design. Figure 21 shows the conceptual design for the linear synthetic aperture imaging system that could be used for imaging during the sluicing operations. The system will use a linear scanner that can pan and

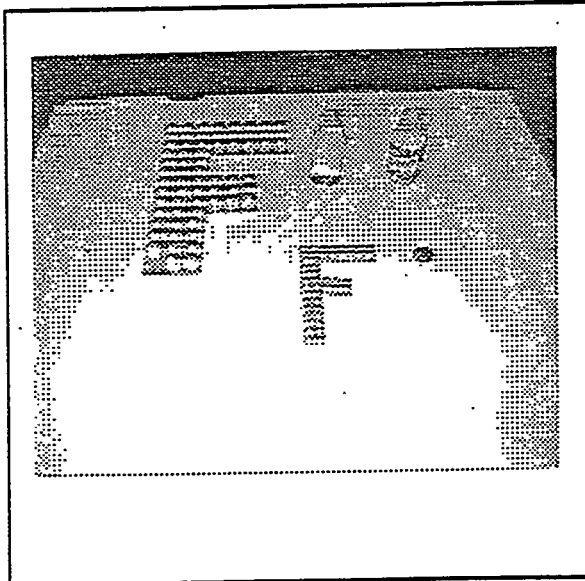


Optical Image

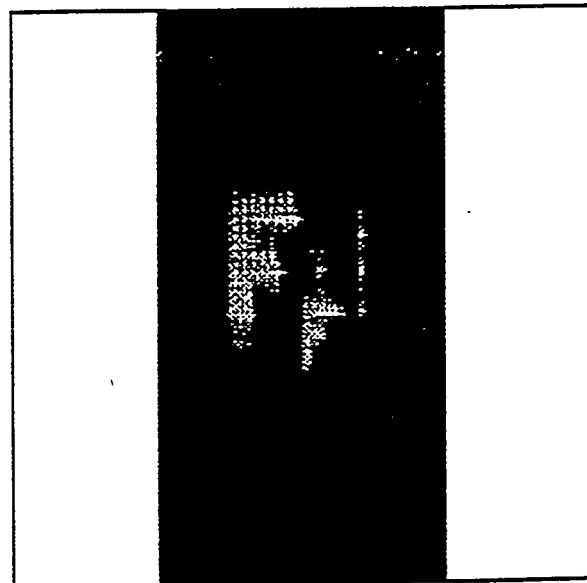


Millimeter Wave Image

FIGURE 18: Millimeter Wave Image of 1.5-In. Diameter Metallized Spheres

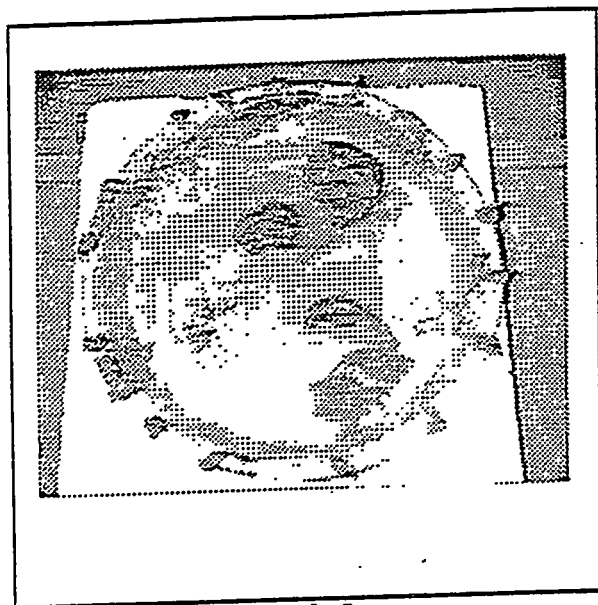


Optical Image



Millimeter Wave Image

FIGURE 19. Millimeter Wave Image of Various Targets



Optical Image



Millimeter Wave Image

FIGURE 20. Millimeter Wave Image of Duct Putty in Wading Pool

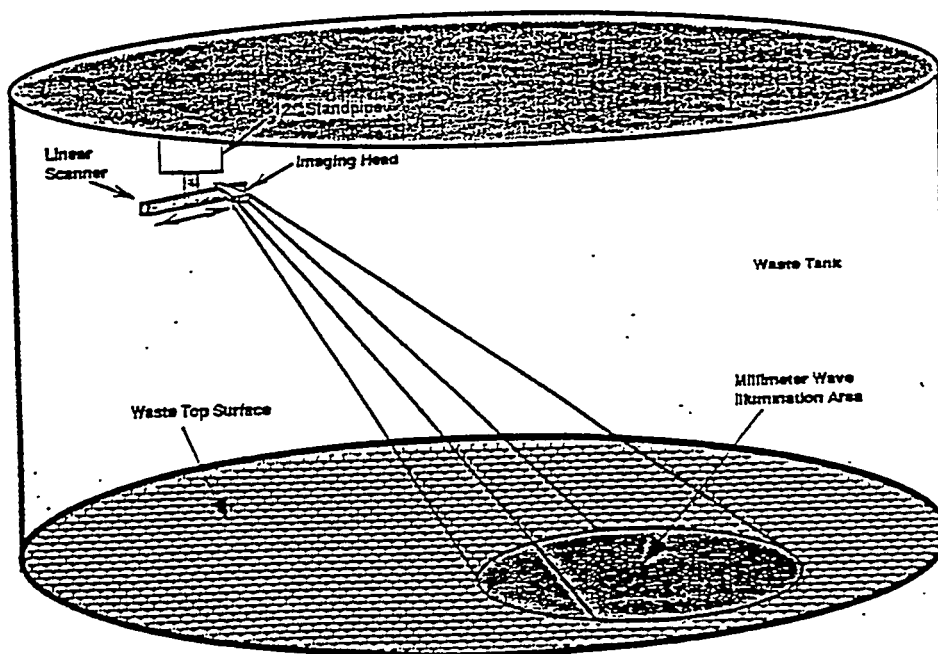


FIGURE 21: Conceptual Design of Millimeter Wave Imaging System for Sluicing Operations

tilt for coverage over the area of the waste tank. The linear array will be approximately two feet long. The imaging system will be capable of updating an image every 30 seconds. Some of the imaging system specifications are shown in Table 14.

The imaging head and linear scanner can easily fit down through the standoff riser in a folded fashion, and will be encased in a radome covering material to allow for decontamination. The millimeter waves easily penetrate through this plastic outer cover. The millimeter wave imaging head can be fabricated into a miniaturized configuration for ease of entrance into the waste tank. The millimeter wave transceiver will be fabricated out of semiconductor diodes and metal waveguide. This will allow for a very rugged imaging system in a high-radiation environment.

Preliminary image focusing software has already been developed. This image forming software can be readily implemented on a PC-based computer with special high-speed computational boards. The PC computer will also control the scanner and display the reconstructed image of the waste tank surface.

TABLE 14. Millimeter Wave Imaging System Specifications

|                      |                  |
|----------------------|------------------|
| Operating Frequency: | 95-115 GHz       |
| Image Frame Rate:    | 1 per 30 seconds |
| Lateral Resolution:  | 1.6 inches       |
| Range Resolution:    | 0.4 inch         |
| Imaging Pixels:      | 256 x 256        |
| F #:                 | 10-20            |

#### 4.0 RADIATION EXPOSURE

The effects of nuclear radiation on the operation of the instruments were not tested in this study. However, during the sluicing operation in the waste tank, the equipment that is placed in the waste tank will be exposed to nuclear radiation for a long period of time. Radiation-tolerant video cameras are commercially available that can withstand an accumulated dose of  $10^8$  R. Recent publications have indicated that charge-injection device (CID) cameras are much more radiation-hardened than CCD cameras (Kaplan 1994). Tests were conducted in this program to compare the sensitivity of a CCD camera to that of a CID camera. The results, shown in Table 15, indicate that the sensitivity of the CID camera was comparable to the sensitivity of the CCD camera. The CID camera that was tested did not have automatic gain control, or any control on the gain, which made it difficult to compare directly to the CCD camera that did have these features.

CCD detectors and other commercial electronic components, such as CMOS preamps, generally begin to fail at about 5000 R (Hubbs et al. 1991, and 1987 CCD Databook 1988). Complete failure of these devices occurs at 30,000 R (Darwish et al. 1988). Radiation-hardened CMOS devices are able to withstand  $10^6$  R (London et al. 1978). However, it has been found that more damage is done to these devices at low dose rates than at high dose rates and that CMOS devices used in low-radiation environments may fail 2-6 times faster than would be predicted by calculating the total exposure (Goben et al. 1990). Silicon photodiodes will withstand  $2 \times 10^8$  R of gamma radiation without degradation (Barnes 1979). Gallium Arsenide, which is the operating diode in the millimeter wave system, will fail between  $75-100 \times 10^6$  R (Witmer et al. 1993).

Sluicing takes a long time to perform, and the equipment may be down in the tank continuously for several months. Thus, shielding of the detector and electronic components will be required of any system placed in the waste tank. The small size and weight of the CCD or CID camera or mm wave antenna tested in this program would allow room for shielding. The system can be enclosed in a lead box, and a mirror can be used to minimize direct shine from the nuclear

**TABLE 15. Comparison of Sensitivity of CCD and CID Cameras**

Target Distance  
40 Feet

| Wavelength<br>Region    | Attenuation*<br>(/ft) |        |        | Visibility*<br>(ft) |     |      | Figure of Merit |       |       |
|-------------------------|-----------------------|--------|--------|---------------------|-----|------|-----------------|-------|-------|
|                         | 25                    | 700    | 1100   | 25                  | 700 | 1100 | 25              | 700   | 1100  |
| Particle Size (Microns) |                       |        |        |                     |     |      |                 |       |       |
| CCD Camera              |                       |        |        |                     |     |      |                 |       |       |
| Visible                 |                       |        |        |                     |     |      |                 |       |       |
| Backlight               | 0.050                 | 0.099  | 0.065  | 60                  | 68  | 103  | 0.67            | 0.59  | 0.39  |
| Frontlight              |                       |        |        |                     |     |      |                 |       |       |
| Room Lights             | 0.076                 | >0.113 | >0.084 | 40                  | <60 | <80  | 1.00            | >0.67 | >0.50 |
| 500 w Bulb              | 0.102                 | >0.113 | >0.084 | 30                  | <60 | <80  | 1.33            | >0.67 | >0.50 |
| CID Camera              |                       |        |        |                     |     |      |                 |       |       |
| Visible                 |                       |        |        |                     |     |      |                 |       |       |
| Backlight               | 0.051                 | 0.085  | 0.065  | 59                  | 79  | 103  | 0.68            | 0.50  | 0.39  |
| Frontlight              |                       |        |        |                     |     |      |                 |       |       |
| Room Lights             | ---                   | 0.085  | 0.078  | --                  | 79  | 86   | --              | 0.50  | 0.46  |
| 500 w Bulb              | 0.100                 | >0.113 | >0.084 | 30                  | <60 | <80  | 1.33            | >0.67 | >0.50 |

\* Attenuation and Visibility measured at 0.63 microns

radiation onto the detector; nuclear radiation will not be reflected from mirrors. As a rule of thumb, one can get about one order of magnitude reduction in damage due to gamma radiation for every inch of lead shielding. There are radiation-tolerant glasses that can withstand  $10^7$  R. Mirrors, lenses, and windows can be designed to be replaced easily during routine servicing.

## 5.0 CONCLUSIONS

Table 16 summarizes the results of this study. The results are stated based on a "figure of merit", which is the ratio of the target distance to the visibility of the fog/water droplets when the target was just visible, using the stated detection/illumination method. The higher the "figure of merit", the better the method is for imaging through the fog/water droplets.

Millimeter wave sensors operating at approximately 94 GHz were able to penetrate the thickest fog/water droplets produced in the test chamber. The amount of millimeter wave attenuation is affected by the size of the water vapor particle--the larger the particle size, the higher the attenuation. The antenna does not have to be large [the antenna used for these tests was approximately 1(W) x 1(H) x 3(L) inches] and could be placed on a scanner to obtain the desired images. The scanner would have to fold out to approximately two feet after being placed down the riser. The millimeter wave sensor operating at 94 GHz was not affected by increasing the conductivity of the fog/water droplets. The millimeter wave system should be able to meet the requirements detailed in this report for viewing through obscurant during a sluicing operation. It is estimated that the hardware to develop a millimeter wave system to be placed in a waste tank would cost (unburdened) approximately \$100K-\$125K. Additional costs would be needed for the deployment system and labor for assembling, testing, and deploying the system. The lateral and range resolution of a millimeter wave system operating at 90 GHz would be 1-2 inches at a range of 40 feet. The image frame rate could be near real-time (one frame every 30 seconds).

Video imaging was not able to penetrate the thickest fog/water droplets. However, it is the least expensive and would require the least amount of technical development, and can be used when the fog/water droplets are not as dense. The density of the fog that can be viewed with video imaging techniques can be 9% to 42% greater, depending on the lighting scheme, by using image enhancement software, which can be done in near real-time. It can also be enhanced by placing lighting near the area to be viewed, instead of placing the lights through the same riser as the camera. Objects could be

**TABLE 16. Comparison of Test Results with Different Sensors**

| Sensor                         | Wavelength<br>(Microns) | Figure of Merit<br>Target Distance |       |       |       |      |      | Notes |
|--------------------------------|-------------------------|------------------------------------|-------|-------|-------|------|------|-------|
|                                |                         | 40 ft                              |       |       | 80 ft |      |      |       |
|                                |                         | Particle Size (Micron)             |       |       |       |      |      |       |
|                                |                         | 25                                 | 700   | 1100  | 25    | 700  | 1100 |       |
| <u>Optical Sensors</u>         |                         |                                    |       |       |       |      |      |       |
| CCD                            | 0.4-1.1                 |                                    |       |       |       |      |      |       |
| Backlighted                    |                         | 0.67                               | 0.59  | 0.39  | --    | ---  | ---  | 1,2   |
| Frontlighted                   |                         | 1.00                               | >0.67 | >0.50 | 1.01  | 0.55 | 0.49 | 1,3   |
| CID                            | 0.4-1.1                 |                                    |       |       |       |      |      |       |
| Backlighted                    |                         | 0.68                               | 0.51  | 0.39  | --    | ---  | ---  | 1,2   |
| Frontlighted                   |                         | --                                 | 0.51  | 0.46  | --    | ---  | ---  | 1,3   |
| Image                          |                         |                                    |       |       |       |      |      |       |
| Intensified                    | 0.4-1.1                 | --                                 | ---   | ---   | --    | ---  | ---  | 1,4   |
| Contrast Enhanced              | 0.4-1.1                 |                                    |       |       |       |      |      |       |
| Backlighted                    |                         | 0.82                               | >0.67 | >0.50 | --    | ---  | ---  | 1,2   |
| Frontlighted                   |                         | 1.29                               | >0.67 | >0.50 | 1.29  | 0.93 | 0.78 | 1,3   |
| Laser Rangefinder              | 0.83                    | 0.73                               | 0.33  | 0.30  | --    | ---  | ---  | 5     |
| Photoconductive                | 0.4-2.2                 | 0.56                               | 0.51  | ---   | --    | ---  | ---  | 1,6   |
| In-Sb                          | 2.0-5.6                 | 1.18                               | 0.30  | 0.30  | 0.85  | 0.31 | 0.21 | 7,9   |
| Hg-Cd-Te                       | 3.2-5.6                 | 0.75                               | 0.19  | 0.24  | 0.50  | 0.12 | 0.07 | 8     |
| Hg-Cd-Te                       | 8-12                    | 1.43                               | 0.23  | 0.14  | 2.00  | 0.24 | 0.15 | 7,9   |
| <u>Acoustic Sensors</u>        |                         |                                    |       |       |       |      |      |       |
| Electrostatic                  | 6600 (50 kHz)           | --                                 | ---   | ---   | ---   | ---  | ---  | 10    |
| Piezoelectric                  | 6600 (50 kHz)           | --                                 | ---   | ---   | ---   | ---  | ---  | 10    |
| Piezoelectric                  | 1500 (215 kHz)          | --                                 | ---   | ---   | ---   | ---  | ---  | 11    |
| <u>Millimeter Wave Sensors</u> |                         |                                    |       |       |       |      |      |       |
| 94 GHz                         | 3190                    | >2.67                              | >0.67 | >0.50 | ---   | ---  | ---  | 12    |

Notes

1. The target for the tests in the visible region was an oxidized steel plate, with a reflectivity of 25% and illuminated with 38 ft-c.
2. Backlighting at 80 feet could not be accomplished with the test set-up.
3. The visual range with frontlighting will decrease as the intensity of the light source increases.
4. Image blooming occurred with the image intensified camera.
5. Backscatter from the fog/water droplets resulted in the loss of range data but images were obtained providing water droplets are at least 16 feet from the rangefinder.
6. An arc lamp was used as the light source in testing this camera. There was no change in the visibility range of the fog/water droplets when the image was viewed in the near infrared.
7. Detector is cooled with liquid nitrogen.
8. Detector is thermoelectrically cooled.
9. This is with target at 10°F above ambient. The target will be visible through denser fog/water droplets as the target temperature increases.
10. The 50 kHz acoustic sensor is affected by noise of air/water movement.
11. The commercial acoustic sensor that was tested did not have enough power to penetrate the fog. Tests indicate that this acoustic sensor would lose 75% of its power travelling to and from a target at 80 feet.
12. The mm-wave sensor operating was able to penetrate the thickest fog/water droplets produced by the test chamber. Attenuation was measured to be 1-8 db for a target at 40 feet.

detected in 50%-100% thicker fog using the frontlighting approach, depending on the intensity of the light source. In a waste tank, frontlighting could be achieved by either placing the lights down a riser near the area undergoing the sluicing operation or placing lights on the robotic arm controlling the water nozzles. There was no gain in using a low light level camera for viewing through the fog/water droplets, viewing in the near-infrared region, and using a mercury lamp as the light source. Adding salt to the fog/water droplets did not change the visibility of the target through the water vapor.

Laser range gating has been successfully used for imaging through murky water. However, no system is commercially available that is able to operate at the short-target distances that will occur in a waste tank. Discussions with SAIC in San Diego, CA, indicate that they believe a system they have developed could be adapted for imaging through fog/water droplets in a waste tank during a sluicing operation. It was not possible within the funding level and time frame of this program to pursue this approach.

Testing with a laser range finder indicated that the instrument loses its ability to determine range information in the fog/water droplets. It was able to obtain an image through the fog at low resolution. The image of a target at 40 feet being equivalent to the video image of a target at 80 feet. With water droplets, an image was obtained, providing that the water droplets were at least 16 feet from the range finder; otherwise, the image exhibits random noise. The laser range finder was able to scan the target area at 40 feet in a few seconds.

Infrared optical techniques do not appear to be viable for viewing through obscurants during a sluicing operation. Although infrared detectors did operate in thicker fog than visible techniques, they exhibited higher attenuation in water droplets. In addition, a system that does not require liquid nitrogen cooling operated only marginally better than a video system operating in the visible wavelength regions. Finally, because of the small temperature differences between the target and the background, the image may not correlate exactly with the surfaces in the waste tank.

Acoustic sensors would need to be operated at high power in order to be used for this application. At 215 kHz, 75% of the power of the beam would be lost in the fog in the round-trip travel to a target 75 feet away. In addition, acoustic sensors must operate at a frequency above the ambient acoustic noise due to the sluicing operation in the waste tank. Sensors tested at 50 kHz were affected by the noise of air movements.

## 6.0 RECOMMENDATIONS

Test results from this program will provide a basis to determine the best method to view through the fog/water droplets in a waste tank during a sluicing operation. The best method will be governed by the density of the fog/water droplets. Testing indicated that millimeter wave sensors were able to penetrate the thickest fog/water droplets, and were not affected by the conductivity of the fog/water droplets. If it is important to image through a very dense fog, then funding should be provided for further development of this sensor for specific applications. A system should be developed and tested in a waste tank during a sluicing operation.

Other methods may also be viable. Laser range gating, although not tested in this program, may be another method that could be used for imaging during sluicing operations. If alternative methods to using millimeter wave technology to image through dense fog/water droplets is desired, then funding should be provided to a manufacturer of a laser range gated system to update their system for the short-target distances that would occur in a waste tank. Then this system can be tested in the fog/water droplet test fixture developed in this program to determine the feasibility of this approach.

If the fog/water droplets are not too dense, video imaging is the least expensive and requires the least amount of technical development. Frontlighting is beneficial for a high density of fog/water droplets, and this approach should be considered. Software developed for image enhancement will extend the range for viewing through the fog/water droplets. These methods should also be pursued if the fog/water droplets are not as dense and the cost of developing more sophisticated systems is prohibitive.

The choice of the best system that can be used in a specific waste tank is dependent on measuring the conditions in the waste tank (e.g., How dense is the fog/water droplets in the waste tank?). If it is important to image through the fog/water droplets in the atmosphere in a tank, then funding is needed to obtain information about the conditions in the waste tank in order to produce a system that will meet the sluicing requirements.

## 7.0 REFERENCES

- 1987 CCD Databook CCD Solid State Imaging Technology. Fairchild Weston Systems, Inc., 1988.
- Barnes, C. E. 1979. "Radiation Effects in InGaAs LED's and Si Photodiodes." J. Appl. Phys. 50(8):5242-5250.
- Block, Judith ed. 1993. Lighting Handbook, 8th Ed., Illuminating Engineering Society of North America, pp. 93-96.
- Darwish, Mohamed N., Martin C. Dolly, Charles A. Goodwin, and Jeffrey L. Titus. 1988. "Radiation Effects on Power Integrated Circuits." IEEE Transactions on Nuclear Science. 35(6):1547-1551.
- Goben, C. A., and W. E. Price. 1990. "Failures of CMOS Devices at Low Radiation-Dose Rates." NASA Tech Briefs, p. 30.
- Hockey, R. L. 1993. Electromagnetic Moisture Measurement in Waste Tank Simulants and Ionic Solutions. Letter report of Work Performed for Westinghouse Hanford Company.
- Hubbs, J. E., G. A. Dole, M. E. Gramer, and D. C. Arrington. 1991. "Radiation Effects Characterization of Infrared Focal Plane Arrays Using the Mosaic Array Test System." Optical Engineering. 30(11):1739-1744.
- Kaplan, Herbert. 1994. "CID Imagers Handle The Hard Stuff." Photonics Spectra, p. 42.
- London, A., and R. C. Wang. 1978. "Dose Rate and Extended Total Dose Characterization of Radiation Hardened Metal Gate CMOS Integrated Circuits." IEEE Transactions on Nuclear Science. ns-25(6):1172-1175.
- Peters, T. J., W. R. Park, W. M. Lechelt, and J. C. Spanner. 1991. Evaluation of Acoustic Sensors for Single-Shell Storage Tanks: Laboratory Test Phase. Report of work performed for Westinghouse Hanford Corporation.
- Soumekh, M. 1991. "Bistatic Synthetic Aperture Radar Inversion with Application in Dynamic Imaging," IEEE Transactions on Signal Processing. 39(9):2044-2055.
- Spraying Systems Co. product literature. 1981. Comparative Particle Size Data for SSCO Spray Nozzles and Rain Drop Particle Size Table (40 PSI).
- Weast, Robert C., ed. 1976-1977. Handbook of Chemistry and Physics, 57th ed., CRC Press, Cleveland, OH 44128.

Witmer, S. B., S. D. Mittleman, D. Lehy, F. Ren, T. R. Fullowan, R. F. Kopf, C. R. Abernathy, S. J. Pearton, D. A. Humphrey, R. K. Montgomery, P. R. Smith, J. P. Kreskovsky, and H. L. Grubin. 1993. "Effects of Ionizing Radiation on GaAs/AlGa As and InGaAs/AlInAs Heterojunction Bipolar Transistors." Materials Science & Engineering B: Solid-State Materials for Advanced Technology. G20(3):280-291.

APPENDIX A

GLOSSARY OF TERMS

## APPENDIX A

### GLOSSARY OF TERMS

1. Active Illumination: An energy source, e.g., a laser beam, is scanned across a target area, and the energy reflected from the target is detected in order to determine the profile of the target area (see Figure A1).
2. Backlighted: An energy source, e.g., an arc lamp, is projected to a target area through the fog/water droplets (see Figure A2).
3. Figure of Merit: A method to compare different tests relative to each other. It is the ratio of the actual target distance to the visibility of the fog/water droplets. The larger the figure of merit, the better is the detection/illumination scheme for imaging through the fog/water droplets.
4. Frontlighted: An energy source, e.g., an arc lamp, is placed near the target area in order to illuminate the target (see Figure A3).
5. Optical Attenuation: The decrease in the power of an energy beam as it travels through a media, e.g., fog/water droplets. The attenuation of the media can be calculated by:

$$a = -\ln(I/I_0)/x$$

where  $a$  = attenuation coefficient of the media

$I$  = intensity of energy beam at a certain distance ( $x$ ) into the media

$I_0$  = intensity of energy beam before entering the media

6. Passive Emission: The energy emitted from a target area is detected in order to determine the profile of the target (see Figure A4).
7. Visibility: The distance an object can be seen through a media, e.g., fog/water droplets. It is calculated by the equation:

$$V = -\ln T/a$$

where  $V$  = visibility of the atmosphere

$T$  = transmittance of light source (laser beam) through the atmosphere

$a$  = attenuation of atmosphere

8. Visual Range: The same as visibility of an object.

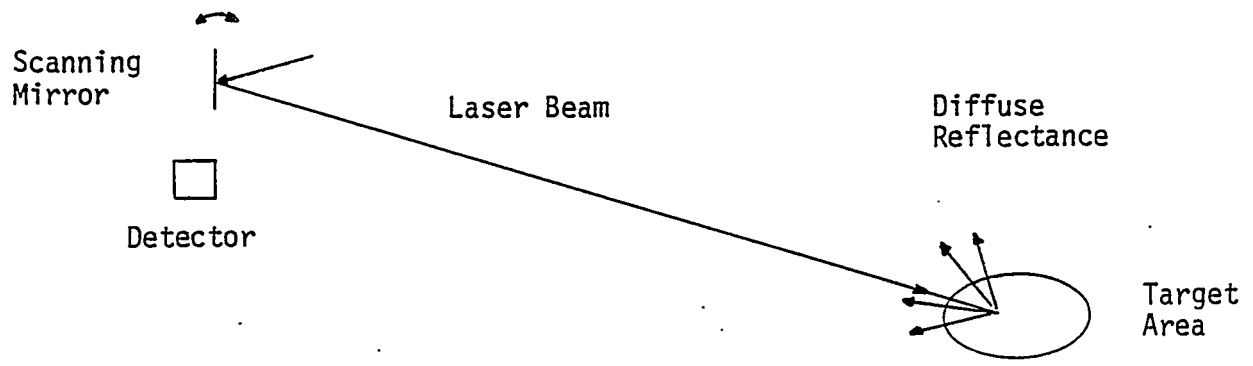


FIGURE A1: Active Illumination

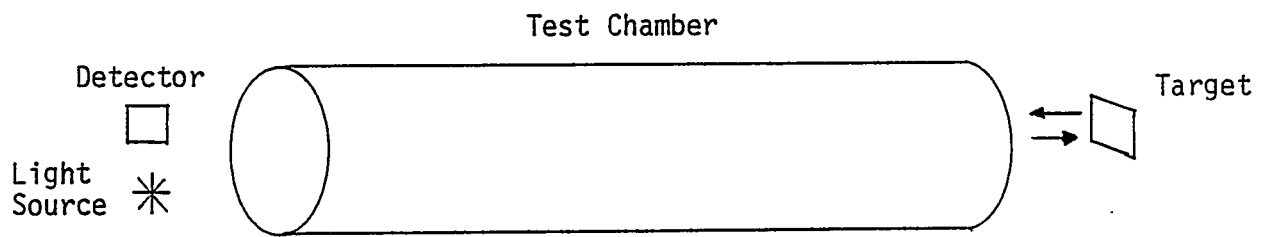


FIGURE A2: Backlighting

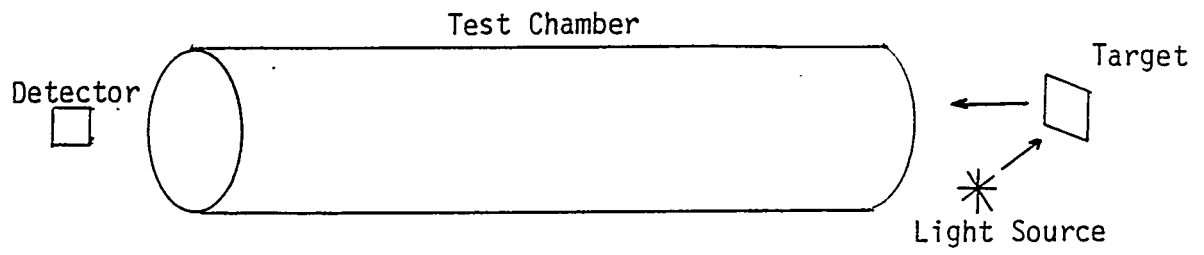


FIGURE A3: Frontlighting

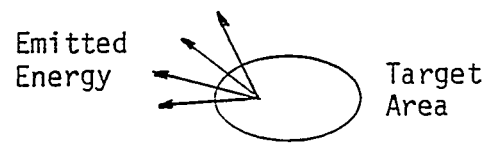
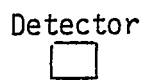


FIGURE A4: Passive Emission

APPENDIX B

LIST OF DETECTION EQUIPMENT

APPENDIX B

LIST OF DETECTION EQUIPMENT

Optical Detection Devices

| Wavelength Region                                                  | Manufacturer                         | Model No.              |
|--------------------------------------------------------------------|--------------------------------------|------------------------|
| 0.4-1.1 Micron<br>(Silicon Detector)                               |                                      |                        |
| CCD                                                                | Cohu Inc.                            | 6500                   |
| CID                                                                | CID Technologies, Inc.               | CID2250E               |
| Image Intensified                                                  | ITT Electro-Optics Products Division | E4577-00100            |
| 0.83 Micron                                                        | Perceptron                           | Laser                  |
| 0.4-2.2 Micron<br>(Composite PbO and PbS Photoconductive Detector) | Electro-Physics                      | MicroViewer 7290       |
| 2.0-5.6 Micron<br>(In-Sb Detector)                                 | AGA Corporation                      | 680/102B               |
| 3.2-5.6 Micron<br>(Hg-Cd-Te Detector)                              | Hughes Aircraft Company              | Probeye TVS Model 7300 |
| 8-12 Micron<br>(Hg-Cd-Te Detector)                                 | Inframetrics Inc.                    | 600L                   |

Acoustic Sensors

| Frequency                  | Manufacturer             | Model No.        |
|----------------------------|--------------------------|------------------|
| 50 kHz<br>(Electrostatic)  | Polaroid Inc.            | (Evaluation Kit) |
| (Piezoelectric)            | Lundahl Instruments Inc. | DCU-7            |
| 215 kHz<br>(Piezoelectric) | Micro Switch Inc.        | 942              |

Millimeter Wave Sensors

| Frequency | Manufacturer | Model No. |
|-----------|--------------|-----------|
| 94 GHz    | Millitech    | SGH10     |

APPENDIX C

SAMPLE CALCULATION OF ATTENUATION, VISIBILITY, AND FIGURE OF MERIT

## APPENDIX C

### SAMPLE CALCULATION OF ATTENUATION, VISIBILITY, AND FIGURE OF MERIT

#### Sample Calculation

A helium neon laser was placed on one end of the test chamber, and a photodetector was placed on the other end of the chamber so that the laser beam transversed through the test chamber. The intensity of the helium neon laser beam was first measured with no fog/water droplets in the chamber. For this example, assume it was 2.5 mw. Next, the test chamber was filled with fog/water droplets until the target could barely be seen using a given detector/illumination method. At this point, the power of the transmitted laser beam was measured. For this example, assume it was 0.5 mw. Then, the transmission of the fog/water droplets was:

$$T = I/I_0$$

where  $T$  = transmittance of the laser beam

$I$  = intensity of the laser beam through the fog/water droplets

$I_0$  = intensity of the laser beam with no fog/water droplets in the chamber

In this case:  $T = 0.20$

Then the attenuation of the fog/water droplets can be calculated by:

$$a = -\ln T/x$$

where  $a$  = attenuation coefficient of the laser beam through the fog/water droplets

$x$  = distance the laser beam travelled through the fog/water droplets

For these tests,  $x = 40$  feet. Therefore, for this example,  $a = 0.040/\text{foot}$ .

The visibility of the fog/water droplets can then be calculated using this same equation (Block 1993). It was experimentally determined that an

oxidized steel plate (reflectivity = 25%), illuminated by room lights (408 lux, or 38 ft-c), was just visible by the naked eye when the transmittance of the laser beam was 0.049 in the fog and 0.0012 in the water droplets. Then, the visibility of the atmosphere is given by:

$$V = -\ln T/a$$

where  $V$  = visibility of the atmosphere  
 $T$  = transmittance of the laser beam  
 $a$  = attenuation of the atmosphere

For the example being illustrated in this appendix, the visibility of the fog is:  $V = -\ln (0.049)/0.040 = 75$  feet. From this, a "figure of merit" of the detection/illumination scheme can be calculated. If we assume that the target was 40 feet from the detector, then: "Figure of merit" =  $40/75 = 0.53$ . A "figure of merit" of unity would mean that the target (an oxidized steel plate illuminated by room lights) could be detected by the detection/illumination scheme at the same distance as it could be barely seen by the naked eye. If the "figure of merit" is greater than unity, then the target could be detected before it could be visibly seen. The larger the "figure of merit", the better the detection/illumination scheme is for imaging through fog/water droplets.

APPENDIX D

MILLIMETER WAVE IMAGING THEORY

## APPENDIX D

### MILLIMETER WAVE IMAGING THEORY

#### DATA COLLECTION

Image data is gathered by scanning a side-looking transceiver along a linear aperture and illuminating a stationary target or image region, as shown in Figure D1. The transceiver is assumed to have a spherical radiation pattern; therefore, the entire target region may be illuminated from each position along the synthesized aperture. Wideband data is gathered with frequency  $\omega$  ranging from  $\omega_1$  to  $\omega_2$ , where there is no restriction on the width of the frequency band. An aperture of length,  $D$ , is synthesized along  $x'$  from  $-D/2$  to  $D/2$ . In Figure D1, the primed coordinates  $(x',y')$  are used to denote the transceivers coordinates, and the unprimed coordinates  $(x,y)$  are used to denote the target or image coordinates.

The measured data will be the superposition integral of the target reflectivity function times a complex phase factor due to the round-trip propagation delay.

$$s(x', \omega) = \iint f(x, y) e^{j2k\sqrt{(x-x')^2+y^2}} dx dy \quad (1)$$

Where  $f(x,y)$  is the target reflectivity function and  $k=\omega/c$  is the wavenumber. Slow amplitude variation due to spherical spreading is ignored since it may be easily compensated for in the raw data.

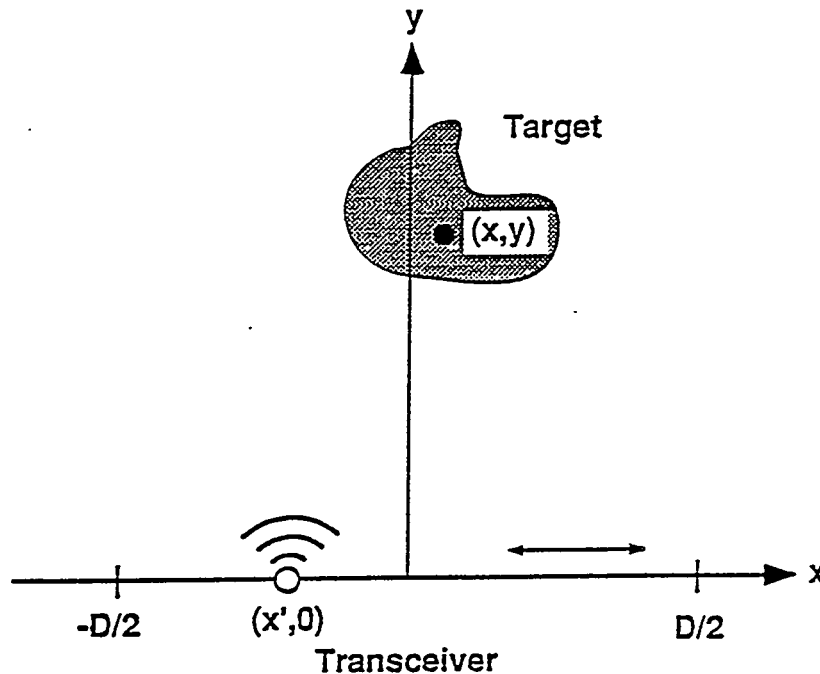


FIGURE D1: Synthetic aperture data collection configuration.

## IMAGE RECONSTRUCTION

The spherical wave in (1) may be decomposed into plane wave components using the following relation,

$$e^{j\omega k\sqrt{(x-x')^2+y^2}} = \int e^{j(k_x'(x'-x) - \sqrt{4k^2 - k_x'^2}y)} dk_x' \quad (2)$$

where  $k_x$  is the spatial wavenumber along the  $x'$  coordinate and ranges from  $-2k$  to  $2k$  for propagating waves. Using (2), the measured data  $s(x', \omega)$  can be expressed as

$$s(x', \omega) = \iint \iint f(x, y) e^{-j(k_x'x + \sqrt{4k^2 - k_x'^2}y)} dx dy \left] e^{jk_x'x'} dk_x' \quad (3)$$

The two-dimensional Fourier Transform is defined by

$$G(k_x, k_y) = \iint g(x, y) e^{-j(k_x x + k_y y)} dx dy \equiv FT_{2D}\{g(x, y)\} \quad (4)$$

and its inverse by

$$g(x, y) = \frac{1}{(2\pi)^3} \iint G(k_x, k_y) e^{j(k_x x + k_y y)} dk_x dk_y \equiv FT_{2D}^{-1}\{G(k_x, k_y)\} \quad (5)$$

Examination of (3) reveals a two-dimensional Fourier Transform,

$$\iint f(x, y) e^{-j(k_x'x + \sqrt{4k^2 - k_x'^2}y)} dx dy = FT_{2D}\{f(x, y)\} \equiv F(k_x', \sqrt{4k^2 - k_x'^2}) \quad (6)$$

Simplifying (3) yields,

$$s(x', \omega) = \int F(k_x', \sqrt{4k^2 - k_x'^2}) e^{jk_x'x'} dk_x' \quad (7)$$

This relation can be inverted by applying the one-dimensional Fourier Transform with respect to  $x'$  to both sides of (7),

$$\int s(x', \omega) e^{-jk_x'x'} dx' \equiv S(k_x', \omega) = F(k_x', \sqrt{4k^2 - k_x'^2}) \quad (8)$$

This equation is simplified further by applying

$$k_x^2 + k_y^2 = (2k)^2 \quad (9)$$

$$w = \frac{c}{2} \sqrt{k_x^2 + k_y^2} \quad (10)$$

$$k_x' = k_x \quad (11)$$

$$k_y = \sqrt{4k^2 - k_x^2} \quad (12)$$

to obtain

$$F(k_x, k_y) = S\left(k_x, \frac{c}{2} \sqrt{k_x^2 + k_y^2}\right) \quad (13)$$

Thus, samples of the two-dimensional Fourier Transform of the reflectivity function are obtained from samples of the wideband data after this data has been Fourier Transformed in the  $x$  direction. Typically, data will be gathered at uniformly spaced  $x$  positions and at uniform frequency intervals. After the raw data has been Fourier Transformed in the  $x$ -direction, the data will be uniformly sampled in  $k_x$  and  $\omega$ . In order to obtain uniform samples in the  $k_x, k_y$  domain, interpolation between frequency samples is necessary.

The target reflectivity function is found by the inverse two-dimensional Fourier Transform,

$$f(x, y) = FT_{2D}^{-1}\{F(k_x, k_y)\} \quad (14)$$

The magnitude  $f(x, y)$  is then displayed as the image.

## RESOLUTION

The expected resolution for the wideband system is defined by the width of the synthetic aperture (or the illuminated aperture defined by the antenna beamwidth) and by the frequency bandwidth. In the lateral direction, the expected resolution is given by

$$\delta_x = \frac{\lambda_c}{2} \frac{r}{L} \quad (15)$$

Where  $\lambda_c$  is the wavelength at the center frequency,  $r$  is the distance to the target, and  $L$  is the lesser of the width of the aperture or  $r$  times the antenna beamwidth. In the range direction, the expected resolution is given by

$$\delta_y = \frac{c}{2B} \quad (16)$$

Where  $c$  is the speed of light and  $B$  is the bandwidth of the measured image data. If a slant plane geometry is used then the resolution is degraded to

$$\delta_y = \frac{c}{2B} \frac{1}{\sin\theta_{slant}} \quad (17)$$

Where  $\theta_{slant}$  is the slant angle. Image distortion due to the slant plane geometry is readily compensated for by a simple mapping of the reconstructed image from the slant plane to the target plane.

### FREQUENCY AND SPATIAL SAMPLING

The required frequency sampling increment is determined by the following relation

$$\Delta f \leq \frac{1}{(2R_{max}/c)} \quad (18)$$

Where  $R_{max}$  is the furthest range extent in the returned data. If a frequency increment larger than this is used, the Nyquist sampling criterion will not be satisfied and the data will be undersampled. The consequence of this is that targets beyond the unaliased range,  $R_{max}$ , will wrap-around and appear in the reconstructed image.

The spatial sampling required along the linear synthetic aperture is

$$\Delta x \leq \frac{\lambda_{min}}{4} \quad (19)$$

This limit guarantees sampling that satisfies the Nyquist criterion of at least 2 samples per spatial wavelength for any direction of wave propagation (up to  $\pm 90^\circ$ ). If directional antennas are used that limit the direction of propagation to significantly less than  $90^\circ$  then this sampling interval may be increased. The consequence of inadequate sampling in the x-direction is that aliasing will occur with wrap-around of image features in the x-direction.

### PHASE AND AMPLITUDE CALIBRATION

Practical millimeter-wave and other transceivers will often require calibration in order to maintain high phase and amplitude accuracy. Fortunately, this type of calibration can typically be performed as port-processing in the computer, rather than requiring hardware compensation. Phase accuracy is particularly important for imaging applications, since phase errors relate directly to position errors. This ultimately leads to the lack of sharp focus in the reconstructed images.

Calibration can be accomplished by placing a flat plate target at a known distance from the transceiver and recording the phase and amplitude of the wideband data. The measured phase and amplitude are compared with the expected phase and amplitude calculated from the known distance to the target. A table of phase and amplitude corrections is computed from the ratio of the expected and measured returns. This correction can then be applied to subsequent data to calibrate the phase and amplitude of the measured data.

DISTRIBUTION

OFFSITE

| <u>No. of Copies</u> |                                                                                                                                                                        | <u>No. of Copies</u> |                                                                                                                                       |
|----------------------|------------------------------------------------------------------------------------------------------------------------------------------------------------------------|----------------------|---------------------------------------------------------------------------------------------------------------------------------------|
| 12                   | DOE Office of Scientific and Technical Information                                                                                                                     | 6                    | DOE/Office of Waste Management<br>Trevion II Building<br>12800 Middlebrook Road<br>Germantown, MD 20874                               |
| 8                    | DOE/Office of Technology Development<br>Trevion II Building<br>12800 Middlebrook Road<br>Germantown, MD 20874                                                          |                      | S. Domotor EM-35<br>H. F. Walter EM-34<br>J. O. Boda EM-32<br>J. Coleman EM-35<br>S. P. Cowan EM-30<br>L. Harmon EM-32                |
|                      | S. M. Wolf EM-542<br>J. M. Lankford EM-552<br>G. E. Voelker EM-50<br>G. Boyd EM-53<br>S. T. Lien EM-54<br>S. M. Prestwich EM-52<br>W. Schutte EM-54<br>C. Prudy EM-541 |                      | DOE/Office of Waste Operations<br>Forrestal Building<br>U.S. Department of Energy<br>1000 Independence Ave SW<br>Washington, DC 20585 |
| 2                    | DOE/Office of Environmental Restoration<br>Trevion II Building<br>12800 Middlebrook Road<br>Germantown, MD 20874                                                       |                      | J. E. Lytle EM-30                                                                                                                     |
|                      | J. E. Baublitz EM-40<br>J. J. Fiore EM-42                                                                                                                              |                      | DOE/Office of Tech.Dev.<br>Forrestal Building<br>U.S. Department of Energy<br>1000 Independence Ave SW<br>Washington, DC 20585        |
| 2                    | DOE/Office of Restoration & Waste Management<br>Forrestal Building<br>U.S. Department of Energy<br>1000 Independence Ave SW<br>Washington, DC 20585                    |                      | C. W. Frank EM-50                                                                                                                     |
|                      | W. Bixby EM-60<br>L. W. Smith EM-60                                                                                                                                    |                      | DOE/Office of Env. Rest.<br>Forrestal Building<br>U.S. Department of Energy<br>1000 Independence Ave SW<br>Washington, DC 20585       |
|                      |                                                                                                                                                                        |                      | R. P. Whitfield EM-40                                                                                                                 |

No. of  
Copies

G. Allen  
Department 6607/MS 0756  
Sandia National Laboratories  
P.O. Box 5800  
Albuquerque, NM 87185-0756

D. H. Bandy  
U.S. Department of Energy  
P.O. Box 5400  
Albuquerque, NM 87115

J. D. Berger  
Westinghouse Hanford Company  
P.O. Box 1970  
Richland, WA 99352

J. B. Berry  
Oak Ridge National Laboratory  
P.O. Box 2008  
Oak Ridge, TN 37831-6330

W. Bliss  
Environmental Management Div.  
Reynolds Electrical & Eng.  
Co., Inc.  
2501 Wyandotte  
P.O. Box 98521  
Las Vegas, NV 89193-8521

T. M. Brouns  
Pacific Northwest Laboratory  
P.O. Box 999  
Richland, WA 99352

P. Colombo  
Brookhaven National Lab  
Building 830  
Upton, NY 11973

S. Conway  
CCEM  
Colorado Center for  
Environmental Mgmt  
1536 Cole Blvd, Bldg 4, Suite  
180  
Golden, CO 80401

J. Coronas  
AMES Laboratory  
329 Wilhelm Hall  
Iowa State University  
Ames, IA 50011

No. of  
Copies

K. Kibbe  
Martin Marietta Energy Systems  
P.O. Box 2003  
Bldg K-1011, MS 7172  
Highway 58  
Oak Ridge, TN 37831-7172

K. Kostelnik  
EG&G Idaho, Inc. MS 3930  
P.O. Box 1625  
200 South Woodruff  
Idaho Falls, ID 83415-3970

A. P. Malinauskas  
Oak Ridge National Laboratory  
P.O. Box 2008, MS 7122  
Oak Ridge, TN 37831-7172

L. McClure  
WINCO  
Westinghouse Idaho Nuclear Co.  
P.O. Box 4000  
Idaho Falls, ID 83415-2202

K. McWilliam  
U.S. Department of Energy  
Nevada Operations Office  
P.O. Box 98518  
Las Vegas, NV 89109

J. Moore  
J. Sweeney  
U. S. Department of Energy  
Oak Ridge Operations Office  
P.O. Box E  
Oak Ridge, TN 37831

J. Nelson  
Sandia National Laboratories  
P.O. Box 5800, Division 6621  
Albuquerque, NM 87185-5800

K. Nuhfer  
FERMCO  
P.O. Box 398704  
Cincinnati, OH 45239-8704

M. G. O'Rear  
U.S. Department of Energy  
Savannah River  
Operations Office  
RFD #1, Bldg. 703A,  
Rm E208 North  
P.O. Box A  
Aiken, SC 29802

No. of  
Copies

K. Stevenson  
U.S. Department of Energy  
376 Hudson Street  
New York, NY 10014-3621

C. Tsang  
Earth Sciences Division  
Bldg. 50E  
Lawrence Berkeley Laboratory  
Berkeley, CA 94720

D. Trader  
U.S. Department of Energy  
Richland Operations Office  
P.O. Box 550  
Richland, WA 99352

R. Tyler  
U.S. Department of Energy  
Rocky Flats Operations Office  
DOE Building 1166  
Golden, CO 80402-0464

S. Webster  
U.S. Department of Energy  
Chicago Field Office  
9800 South Cass Avenue  
Argonne, IL 60439-4837

T. Wheelis [WM]  
Sandia National Laboratory  
Department 6623  
Albuquerque, NM 87545

T. Williams  
U.S. Department of Energy  
Idaho Operations Office  
785 DOE Place  
Idaho Falls, ID 83402

C. Zeh  
Morgantown Energy  
Technology Center  
3610 Collins Ferry Road  
Morgantown, WV 26507-0880

No. of  
Copies

R. Craig  
HAZWRAP  
P.O. Box 2003, MS 7606  
Oak Ridge, TN 37831-7606

H. A. Dugger  
Kaiser Engineers Hanford  
1200 Jadwin Avenue  
Richland, WA 99352

N. Egan  
Program Development Division  
MSE Inc.  
P.O. Box 3767  
Butte, Montana 59702

D. Emilia  
Strategic Planning Dept.  
Chem-Nuclear Geotech  
P.O. Box 1400  
2597B-3/4 /Road (81503)  
Grand Junction, CO 81502-2567

B. Erdal  
Los Alamos National Laboratory  
MS D446  
Los Alamos, NM 87545

R. L. Gilchrist  
Westinghouse Hanford Company  
P.O. Box 1970  
Richland, WA 99352

J. E. Helt  
Office of Waste Mgt. Programs  
9700 South Cass Avenue  
Argonne, IL 60439-4837

A. C. Heywood  
P.O. Box 808  
7000 East Avenue  
MS L-207  
Livermore, CA 94550

R. Jacobson  
Desert Research Institute  
P.O. Box 19040  
Las Vegas, NV 89132

No. of  
Copies

J. L. Peterson  
EG&G Rocky Flats, Inc.  
P.O. Box 464, Building T130B  
Golden, CO 80402-0464

M. Peterson  
Pacific Northwest Laboratory  
P.O. Box 999  
Richland, WA 99352

P. J. Pettit  
FERMCO  
6025 Dixie Highway, Suite 250  
Fairfield, OH 45014L. Rogers  
EG&G Energy Measurements, Inc.  
P.O. Box 1912, MS RSL-11  
Las Vegas, NV 89125

P. A. Saxman  
U.S. Department of Energy  
Albuquerque Operations Office  
P.O. Box 5400  
Albuquerque, NM 87115

R. Scott  
U.S. Department of Energy  
San Francisco Field Office  
1333 Broadway  
Oakland, CA 94612

S. Slate  
Pacific Northwest Laboratory  
P.O. Box 999  
Richland, WA 99352

G. Staats  
U.S. Department of Energy  
Pittsburgh Energy Technology  
Center  
P.O. Box 10940  
Pittsburgh, PA 15236-0940

J. L. Steele  
Savannah River Site  
SRL, 773 A, A208  
Aiken, SC 29802

S. L. Stein  
Battelle Seattle Research  
Center  
4000 NE 41st Street  
Seattle, WA 98105

No. of  
Copies

2 SAIC  
4161 Campus Point Court  
San Diego, CA 92121-1513

H. R. Hiddleston  
F. P. Johansen

ONSITE

DOE Richland Operations Office

D. E. Trader

8 Westinghouse Hanford Company

S. J. Eberlein  
P. W. Gibbons  
J. M. Henderson  
L. B. McDaniel  
A. F. Noonan  
E. J. Shen  
R. T. Skamser  
J. A. Yount

21 Pacific Northwest Laboratory

D. W. Bennett  
M. A. Chieda  
B. M. Johnson Jr.  
D. L. McMakin  
T. J. Peters (10)  
D. M. Sheen  
Publishing Coordination  
Technical Report Files (5)